Distinct Roles for Human Cytomegalovirus Immediate Early Proteins IE1 and IE2 in the transcriptional regulation of MICA and PVR/CD155 expression.

Up-regulation of NKG2D and DNAM-1 ligands in human cytomegalovirus infected cells: role of the viral immediate early proteins IE1 and IE2 in MICA and PVR expression.

Benedetta Pignoloni[1^], Cinzia Fionda[1^], Valentina Dell'Oste[2], Anna Luganini[3], Marco Cippitelli[1], Alessandra Zingoni[1], Santo Landolfo[2], Giorgio Gribaudo[3], Angela Santoni[1*], Cristina Cerboni[1*].

[1]Department of Molecular Medicine, Istituto Pasteur-Fondazione Cenci Bolognetti, "Sapienza" University of Rome, Rome, Italy.

[2] Department of Public Health and Pediatric Sciences, University of Turin, Turin, Italy.

[3] Department of Life Sciences and Systems Biology, University of Turin, Turin, Italy.

^ These authors equally contributed to the work.

* Email: cristina.cerboni@uniroma1.it; angela.santoni@uniroma1.it

Short title

HCMV, IE proteins and upregulation of activating ligands

Abstract

NKG2D and DNAM-1 are two activating receptors expressed on cytotoxic lymphocytes, and play an important role in the elimination of virally-infected cells. Their ligands (MICA/B and ULBP1-6 for NKG2D, and Nectin-2 and PVR for DNAM-1) are often up-regulated upon cellular stress, including viral infections. However, the molecular mechanisms driving their expression are largely unknown, and most of these molecules have been described to be down-modulated by human cytomegalovirus (HCMV) to avoid host immune surveillance. Here, we show that laboratory and low-passage HCMV strains induced MICA, ULBP3 and PVR upregulation on different cell types, suggesting that viral immunoevasion not always prevails. Ligands were still up-regulated on HCMV-infected cells treated with phosphonophormic acid, an inhibitor of viral DNA replication, indicating that some events in the early phases of infection are involved in ligand increase. Our data show that the major immediate early (IE) proteins IE1 and IE2 differently contribute to MICA and PVR expression. MICA upregulation, at both transcriptional and protein level, was mainly dependent on IE2, able to directly bind MICA promoter on a specific consensus region that we identified. Both IE proteins were instead required for PVR upregulation, with a mechanism independent from the DNA binding activity of IE2. We also investigated the contribution of the DNA damage response (DDR) in ligand expression, since this pathway is activated by HCMV and is implicated in ligand up-regulation. However, DDR was not involved as ligands were still upregulated when ATM, ATR and DNA-PK kinases were silenced in infected cells. Overall, our data suggest that IE-mediated activation of cellular genes stimulating cytotoxic lymphocytes might be crucial for the anti-viral host response, and needs to be better characterized in order to design more specific reagents.

Author Summary

Human cytomegalovirus (HCMV) is a β-herpesvirus whose infection is usually asymptomatic and followed by the establishment of a life-long latency, controlled by the immune system. However, primary infection or reactivation occurring in immunocompromised hosts, such as AIDS or transplanted patients, or in the fetus, results in high levels of morbidity and mortality, and birth defects. To date, HCMV is contrasted with anti-viral drugs that can produce toxic effects or select mutant resistant strains. Therefore, agents able to potentiate anti-HCMV immune responses could represent an alternative approach. NK and cytotoxic T lymphocytes are crucial in controlling viral infections, and they use several receptor/ligand combinations, able to turn on their anti-viral functions. NKG2D and DNAM-1 are important receptors recognizing HMCV-infected cells, though their ligands are often targeted by the virus, that evolved many strategies to resist cytotoxic lymphocyte attack. Here, we instead demonstrate that some of these ligands can be upregulated on distinct cell types infected with different HCMV strains, and identify some of the mechanisms involved. The findings show that the major viral immediate early proteins, IE1 and IE2, enhance the expression of two ligands (MICA and PVR), opening the way to develop new therapeutic approaches potentiating anti-HCMV immune responses.

Introduction

Human cytomegalovirus (HCMV) is a β-herpesvirus with a large dsDNA genome of approximately 230 kbp, and containing more than 200 open reading frames (Murphy and Shenk, curr top microb immunol 2008; Stern-Ginossar N Science 2012). Although the virus is endemic within the human population, it does not usually cause clinically obvious disease upon primary infection of healthy, immunocompetent individuals, but the immune response is unable to clear the virus, which establishes a life-long latency (Sinclair J JGV 2006). Infection often becomes clinically apparent, causing life-threatening diseases in immunocompromised individuals, such as AIDS patients and organ transplant recipients, upon primary infection or reactivation (Mocarski ES and Tan Courcelle C. 2001. In Knipe DM et al. (Eds), Fields Virology 4th ed. Lippincott Williams & Wilkins, Philadelphia, PA). It is also the major viral cause of birth defects, which can culminate in hearing and vision loss, along with various mental disabilities (Schleiss MR. 2008. Curr Treat Options Neurol). Nearly all HCMV infections result in widespread dissemination throughout the body, with diverse cell types supporting productive viral infection, including fibroblasts, epithelial, endothelial and smooth muscle cells (Sinzger C JGV 1995). In addition, the virus induces a plethora of immunomodulatory pathways to subvert the host innate and adaptive immune responses (Mocarski ES Trends Microbiol 2002). Although there have been numerous attempts to develop an effective HCMV vaccine, a successful formulation has not yet been clinically approved. A limited number of anti-viral drugs are available, but long-term treatment is frequently followed by toxic side effects and the emergence of drug-resistant mutants (Khanna R Trends Mol Med 2006). Clearly, additional safe therapeutic agents that limit HCMV replication are desirable, and thinking in terms of agents able to potentiate anti-HCMV immune responses could be an alternative approach.

With this purpose, we investigated if some of the molecules able to activate cytotoxic lymphocytes could be positively regulated following HCMV infection, favoring the recognition and elimination of infected cells. In particular, we analyzed the expression and regulation of NKG2D and DNAM-1 ligands. NKG2D and DNAM-1 (CD226) are two activating immune receptors expressed by all cytotoxic lymphocytes, i.e, NK cells, CD8+ T cells and gamma-delta T cells (Lanier Nat Immunol 2008). NKG2D delivers a potent activating signal and plays a prominent role in the recognition and elimination of infected cells (Lanier Nat Immunol 2008; Champsaur Immunol Rev 2010). Its ligands are the MHC-I-related molecules MICA, MICB, and the ULBP proteins (ULBP1-6), whose expression is highly restricted in normal cells, but can be rapidly up-regulated or induced upon a cellular stress, including a viral infection (Champsaur Imm Rev 2010; Eagle RA 2007 Nat Rev Immunol). DNAM-1 has been shown to be fundamental to NK cell-dependent anti-tumor immunity (Chan 2014; Gilfillan 2008; Iguchi-Manaka 2008; Lakshmikanth 2009), and its role in viral infections is also starting to emerge (Cella 2010; Nabekura 2014). It is a co-stimulatory Ig-like adhesion molecule and its ligands are PVR (CD155) and Nectin-2 (CD112), belonging to the family of nectins and nectin-like proteins (Takai Y 2008 Nat Rev Mol Cell Biol; Fuchs A 2006 Semin Cancer Biol). Upon engagement by its ligands, DNAM-1 promotes leukocyte migration, activation, expansion and differentiation of T cells, as well as effector responses of both NK and T cells (Takai Y 2008 Nat Rev Mol Cell Biol; Fuchs A 2006 Semin Cancer Biol). Because NKG2D and DNAM-1 have an important role in controlling both NK- and T-cell-mediated immunity, it is reasonable that these receptors/ligands forced HCMV to evolve specific strategies of evasion (Lanier Nat Immunol 2008). In fact, much of the work done on NKG2D/DNAM-1 ligands, including our, have been focused on the immunoevasion strategies evolved by HCMV to inhibit their expression (Rossini G 2012

Mediators Inflamm; Wilkinson 2008). HCMV encodes indeed an impressive array of molecules (UL16, UL141, UL142, US18 and US20, US9, miRNA-UL112) that suppress cell surface expression of both NKG2D and DNAM-1 ligands. The outcome of these immune-evasion strategies is an impaired recognition and elimination of HCMV-infected cells by NK cells and other NKG2D+ and DNAM-1+ cells, likely dampening an adequate immune response (Rossini G 2012 Mediators Inflamm; Wilkinson GWG 2008 J Clin Virol 41:206; per US9: Seidel E Cell Reports 2015; Fielding CA, Plos path 2014). Despite these evidences, it is also known that HCMV infection results in the induction of transcripts encoding activating ligands, in particular of NKG2D (Welte SA EJI 2003; Zou Y JI 2005; Eagle RA Hum Imm 2006). Moreover, there are evidences on the ability of viral immediate early (IE) proteins to up-regulate MICA, MICB and ULBP2 ligands at the transcriptional or protein expression level (Venkataraman and Fielding). Thus, there is the possibility that HCMV may at first positively regulate the expression of activating ligands, allowing recognition of infected cells by cytotoxic lymphocytes and thus a certain level of immune surveillance against the virus, at a time before late immunoevasion genes exert their effects.

IE proteins play an important role in the very early phases of the infection, as they are the first proteins to be expressed during HCMV lytic infection, before early (E) and then late (L) gene products are expressed (Sinclair J JGV 2006). The most abundantly expressed proteins are the 72-kDa IE1 and the 86-kDa IE2 proteins (IE1 and IE2 from now on), together with the other IE protein, known as IE55 (IE2-55). IE proteins are expressed in the absence of *de novo* protein synthesis, are all produced from differentially spliced transcripts, and share the first 85 aminoacids, so that the N-terminal part is identical. However, the remaining sequences differ and likely account for the divergent activities exhibited by each protein (Castillo JP Gene 2002;

Stinski MF Curr Top Microbiol Immunol 2008). IE1 and IE2 initiate the virus productive infection, and they are absolutely critical for the temporal cascade of viral gene expression, as they are known to transactivate E and L genes (Mocarski 2001, Stinski and Meier 2007), and either positively or negatively autoregulate their own expression (Stinski MF, Isaacson MK, or Gibson W Curr Top Microb Imm, 2008). Moreover, while IE1 alone is a relatively weak transactivator and only affects a limited number of promoters that have been tested, IE2, considered to be the most important regulatory protein codified by the virus, is a strong transcriptional activator of cellular gene expression (Stinsky and Meier, Immediate-early viral gene regulation and function; in Human Herpesviruses: Biology, Therapy, and Immunoprophylaxis. Cambridge: Cambridge University Press; 2007) and seems to operate at the promoter level by different mechanisms. It is able to bind DNA directly, repressing its own promoter (Lang and Stamminger JV, 1993), and it binds to several cellular transcription factors via protein-protein interactions, crucial for transcriptional activation of viral and host genes, and for the regulation of vital cellular functions (Stinski MF Curr Top Microbiol Immunol 2008).

Among the cellular pathways activated by IE proteins there is the DNA damage response (DDR) (Castillo 2005, Xiaofei 2011), involved in cell-cycle checkpoint control, DNA replication, DNA repair and apoptosis (Jackson SP, Nature 2009). DNA must be protected from damage produced spontaneously during DNA replication or other physiological processes, as well as after exposure to external stimuli and DNA-damaging agents. Therefore, to maintain genome integrity and avoid mutated DNA duplication, cells respond with a complex series of cellular stress-induced pathways to detect and repair DNA lesions. Likewise, infection by several viruses, including herpesviruses, is sufficient to activate some or all of the DDR-mediated repair pathways. Simplistically, this was perceived as recognition by the host cell of the incoming

genetic material as its own damaged DNA, but it is now considered to be, at least in part, an anti-viral response aimed at combating the pathogen by posing a threat to viral genome integrity and replication (Sinclair A, Expert Rev Mol Med 2004). On the other hand, DNA viruses create nuclear environments beneficial to viral DNA replication through interactions with host proteins, likely to rely on cellular repairing machineries to facilitate successful viral DNA replication (Chaurushiya MS DNA Repair 2009; Xiaofei E Plos Pathogens 2011 and JV 2014). Therefore, many viruses require DDR activation for a fully permissive infection (Turnell AS JGV 2012; Xiaofei E Viruses 2014), and also HCMV induces a strong DDR and activation of multiple markers of this pathway, including ATM, ATR and the downstream protein H2AX. The functional relevance of DDR in HCMV replication is however unclear and controversial results have been published (Shen YH 2004 Circ Res; Castillo JP 2005 J Virol; Gaspar M 2006 PNAS; Luo MH 2007 JV; Xiaofei E 2011 Plos Pathog; Xiaofei E JV 2014; Li R Cell Host Microbe 2011). Noteworthy, DDR is also involved in NKG2D and DNAM-1 ligand expression. In fact, several works including ours demonstrated that expression of MICA, MICB, ULBP1-3 and PVR is in part dependent on the activation of the DDR and on ATM/ATR kinases (Gasser Nature 2005; Cerboni Blood 2007; Soriani Blood 2009; Ardolino Blood 2011; Zingoni Frontiers Immunol 2012). However, it is unknown how HCMV modulates the expression of NKG2D and DNAM-1 ligands in relation to DDR activation. Our study aimed at investigating this aspect, in an attempt to shed light into the involvement of virus-induced DDR pathway in ligand regulation. We also extended our study on the role of IE proteins on NKG2D and, for the first time, DNAM-1 ligand regulation, deepening the molecular mechanisms by which these viral proteins may act on activating ligand expression. These aspects may shed light into some of the mechanisms and molecules stimulating anti-viral immunity against HCMV.

Results

1. Modulation of NKG2D and DNAM-1 ligand expression by different HCMV strains in various cell types.

Increased or *de novo* expression of T/NK cell activating ligands on the plasma membrane of infected cells represents a crucial host immune defense mechanism to sense and react against a wide variety of pathogens (Lanier LL, Nat Imm 2008; Ferrari de Andrade L, Immunology and cell biology, 2014). It is known that HCMV regulates the expression of NKG2D and DNAM-1 ligands, but different and sometimes contradictory results have been reported so far.

Therefore, we first wanted to recapitulate the expression of NKG2D and DNAM-1 ligands on the surface of HCMV-infected cells. We thus initially infected human primary foreskin fibroblasts (HFF) with the laboratory strain AD169, and monitored by immunofluorescence and flow cytometry for NKG2D and DNAM-1 ligand expression, at different days post-infection (dpi) (Figure 1). Uninfected HFFs showed undetectable MICA, MICB, ULBP1 and ULBP4 cell surface expression, but while no MICB, ULBP1 and ULBP4 molecules were detected at any time post-infection on the plasma membrane of infected HFFs (Figure 1A and data not shown), MICA was significantly induced by HCMV already at 1 dpi, with a peak at 3-4 dpi (Figure 1). Increased levels of ULBP3 were also observed on the cell surface of infected fibroblasts, with maximal expression around 3 dpi, while ULBP2 was down-modulated (Figure 1).

When the effect of HCMV infection on DNAM-1 ligands was investigated, a HCMV-mediated upregulation of PVR, but not Nectin-2, was observed, with a significant increase of its cell surface expression, particularly evident around 3 dpi (Figure 1).

Altogether, these results recapitulated but also extended previous findings and showed that

197 infection of HFFs with AD169 caused an increased cell surface expression of MICA, ULBP3 and
198 PVR activating ligands.
199 Since our general aim was at investigating the mechanisms underlying NKG2D and DNAM-1
200 ligand up-regulation, we focused on those molecules that on human primary fibroblasts were
201 either induced or increased by the virus, i.e., MICA, ULBP3 and PVR.
202 To verify that the HCMV-mediated increased expression of MICA, ULBP3 and PVR was not
203 confined to a unique cell type-viral strain combination, and since the highly-passaged strain
204 AD169 has a greater number of genetic differences compared to low-passage strains, including
205 a ~13-15 kb deletion (Cha TA JV 1996; Wilkinson GWG Med Microbiol Immunol 2015), we
206 extended our analysis to other viral isolates and cell types. In particular, we investigated ligand
207 modulation on: i) HFF cells infected with the low-passage strains VR-1814 and TR, and ii)
208 primary endothelial cells (HMVEC) and epithelial cells (ARPE-19) infected with the same strains
209 (Bronzini JV 2012). To this end, mock- and HCMV-infected cells were stained with mAbs
210 specific for MICA, ULBP3 and PVR, and analyzed by immunofluorescence and flow cytometry
211 (Fig. 2). Similarly to what observed on AD169-infected HFFs, we consistently and reproducibly
212 observed an induction of MICA expression on fibroblasts infected with VR-1814, particularly
213 evident at 2-3 dpi (Fig. 2A-B and data not shown). This result was obtained independently from
214 the used MOI (Fig. 2B). Induction of MICA expression was also observed on HFFs infected with
215 another low-passage strain, TR, though to a lower extent (Fig. 2C). However, this observation
216 was confirmed by confocal microscopy analysis, showing that an induced MICA expression was
217 clearly detectable on the cell surface of TR-infected fibroblasts (Fig. S1). When ULBP3 and
218 PVR ligands were examined on HFF cells infected with VR-1814 (Fig. 2A-B) or TR (Fig. 2C), we
219 always observed a statistically significant up-regulation of these molecules as well. Taken

together, these results demonstrated that at 3-4 dpi, MICA, ULBP3 and PVR were up-regulated on the plasma membrane of infected primary fibroblasts in a strain-independent manner.

Next, we extended our investigation to other cell types and HMVECs and ARPE-19 cells were infected with TR and VR-1814 strains (Figure 2C). MICA expression was either down-modulated (on TR-infected HMVECs), or not affected in all other combinations (HMVECs infected with VR-1814; ARPE-19 infected with TR or VR-1814), while ULBP3 and PVR were always up-regulated, independently of the cell type and/or the viral strain used.

Thus, these results demonstrated that, despite few exceptions, HCMV positively regulated the expression of MICA, ULBP3 and PVR activating ligands, with a pattern that generally overcame cellular- or viral strain-related differences.

2. Analysis of the role of the DNA damage response and of ATM, ATR and DNA-PK on HCMV-induced ligand up-regulation and HCMV replication.

Previously, it has been reported that HCMV manipulates the DDR pathway (Castillo JP JV 2005; Luo MH JV 2007; Shen YH Circ Res 2004; Gaspar M and Shenk T PNAS 2006; Xiaofei E PLoS Pathogens 2011), and that DDR activation can regulate NKG2D and DNAM-1 ligand expression (Gasser S Nature 2005; Cerboni Blood 2007; Soriani A Blood 2009; Ward J Plos Pathogens 2009; Richard J Blood 2010; Ardolino Blood 2011; Soriani A JI 2014; Cerboni Frontiers 2014; Fionda C BMC Cancer 2015). Thus, we asked whether DDR was involved in the up-regulation of ligands observed in HCMV-infected cells. To this end, we used different genetic and pharmacological approaches (i.e., gene silencing, use of cells lacking ATM, use of inhibitors), and monitored the effects of inactivating the DDR pathway on MICA, ULBP3 and PVR ligand cell surface levels, as well as on HCMV IE protein expression and viral productive replication (Fig. 3 and Fig. S2-6).

Initially, we verified that the virus-induced activation of the DDR pathway, by measuring the

levels of γH2AX, the phosphorylated form of the histone variant H2AX, a well-known substrate of DDR kinases, including ATM, ATR and DNA-PK (Burma S JBC 2001; Ward IM JBC 2001; Park EJ Nucleic Ac Res 2003). To this end, γH2AX levels were monitored by flow cytometry on mock- or AD169-infected HFFs, at 3 dpi (Fig. S2). Although γH2AX was present in uninfected cells, its levels increased of approximately two-fold upon HCMV infection, demonstrating activation of the DDR pathway in our experimental settings.

Next, we determined the contribution of the three main kinases of the DDR signaling pathway, ATM, ATR and DNA-PK, on ligand expression, IE expression and viral replication. The contribution of ATM was firstly investigated in fibroblasts derived from a patient affected by ataxia-telangiectasia (AT-/-) that do not express detectable levels of the ATM protein (data not shown). Upon HMCV infection, the absence of ATM did not compromise MICA, ULBP3 and PVR expression, as the virus still induced an increased expression of all the three ligands, though with delayed kinetics compared to HFFs, with a peak of expression at 7 dpi (Fig. S3). Moreover, both progeny virus production and IE expression were only partially affected by the absence of ATM. In fact, compared to HFFs, the production of infectious virus, measured by plaque assays, was reduced of approximately 1 to 2 log, from day 3 to day 7 post-infection (data not shown), while the percentage of IE+ cells, analyzed by flow cytometry, was almost overlapping with HFFs (data not shown). These results suggested that functional ATM, though required for optimal infectious virus production (Xiaofei E, PLos Pathogens 2011), is dispensable for the HCMV-mediated up-regulation of MICA, ULBP3 and PVR expression.

Since there is a concern with using AT-/- fibroblasts as a model because the prolonged absence of a functional ATM in cells from AT patients may have resulted in secondary genetic and/or biochemical changes that in turn could alter cellular environments and thereby influence HCMV

replication, we addressed the same issue by using specific siRNA to transiently deplete ATM protein levels (siATM). To this end, HFFs were transfected with siATM or with a non-targeting siRNA (siCtrl) 24 h prior to HCMV infection, and ligand expression, viral replication and gene expression were monitored at 2 dpi (Fig. S4). Similarly to what we observed in AT-/- fibroblasts, transient depletion of ATM did not affect MICA, ULBP3 and PVR expression induced by HCMV infection (Fig. S4A), and it did not significantly compromise either the percentage of IE+ cells or viral replication (Fig. S4C-D). Similar results were obtained with siRNA specific for ATR (Fig. S5) or DNA-PK (Fig. S6).

Finally, we performed a triple gene silencing, by transfecting HFFs with the three siRNA specific for ATM, ATR and DNA-PK (siDDR; Fig. 3). We observed a pattern similar to the one observed by using single siRNA, with no significant modulation of MICA, ULBP3 and PVR (Fig. 3A), despite the three siRNA had a strong inhibitory effect on the protein levels of their respective target kinases (Fig. 3B). Similarly, activating ligands were still up-regulated in AD169-infected HFFs treated with caffeine (data not shown), a well-known and broad spectrum inhibitor of the DDR signaling pathway (Sarkaria JN, Canc Res, 1999; Block WD Nucleic acid Res, 2004). Of note, in triple siRNA-transfected cells we observed a reproducible, though not statistically significant, higher percentage of IE+ cells (Figure 4C) and viral titers (Fig. 3D). This could result from the inhibition of the DDR-dependent cellular host response against HCMV, caused by the triple silencing, which may allow an improved virus replication, less counteracted by DDR kinases (Fig. 3C-D).

Altogether, these results suggest that DDR activation was not required for the HCMV-induced up-regulation of MICA, ULP3 and PVR.

3. The HCMV-induced MICA, ULBP3 and PVR expression depends from events occurring prior to the onset of viral DNA replication.

In order to identify the molecular mechanisms underlying ligand up-regulation in infected cells, and since it has been suggested that IE proteins may positively regulate MICA/B expression (Venkataraman JI 2007; Andresen JI 2007; Fielding Plos Pathogens 2014), we hypothesized that some early events in the early stages of infection could be responsible for ligand increase. To verify this hypothesis, HFFs were infected with HCMV and soon after virus adsorption, phosphonoformic acid (PFA), a selective inhibitor of the viral DNA polymerase (Tyms AS JGV 1987), was added. Expression of ligands was then assessed at 3 dpi. As shown in Fig. 4, MICA, ULBP3 and PVR levels were increased on the surface of infected cells even in the presence of PFA, thus indicating that viral DNA replication and late gene expression are dispensable for ligand up-regulation.

4. HCMV infection increases MICA and PVR mRNA expression.

The results obtained with PFA suggested that expression of viral IE and/or E genes was necessary and sufficient for up-regulation of MICA, ULBP3 and PVR expression. Then, we investigated whether the observed up-regulation of ligands was a consequence of a virus-induced transcriptional activation. We focused on MICA and PVR, as prototype ligands of NKG2D and DNAM-1, respectively, and their mRNA content was measured in infected HFFs by real-time PCR at 6, 12, 24 and 48 hours post-infection (hpi). As shown in Fig. 5, MICA-specific mRNA progressively increased by 48 hpi up to approximately 8-fold the amount present in mock-cells at 48 hpi. Expression of PVR mRNA, whose kinetics in HCMV infected cells is shown here for the first time, was increased as well upon infection, with a maximum of about

2.5-fold at 48 hpi.

These data indicate that the up-regulation of MICA and PVR cell surface levels by HCMV infection is the outcome of a transcriptional activation of the corresponding genes.

5. HCMV IE proteins up-regulate MICA and PVR expression and promoter activity.

Given the observation that early steps of infection were crucial for ligand up-regulation, we hypothesized that the main viral IE proteins – IE1 (IE1-72) and IE2 (IE2-86) - could have a role in the modulation of MICA and PVR expression, since they are known as transcriptional activators of both viral and cellular genes (Castillo and Kowalik, Gene 2002; Stinski and Petrik, Curr. Top Microbiol. Immunol. 2008). Though IE proteins may positively regulate MICA/B expression (Venkataraman JI 2007; Andresen JI 2007; Fielding Plos Pathogens 2014), the molecular mechanisms mediating the modulation of MICA by IE proteins, as well as the contribution of each IE protein, remain unknown. In addition, no information are available about the effect of IE proteins on the expression of other activating ligands, including PVR.

To address this issue, we investigated whether IE1 and IE2 proteins regulate MICA and PVR expression, by transducing HFFs with recombinant adenoviruses (AdV) encoding for IE1, IE2, or for LacZ as a control. Transduction experiments were carried out with a single Adv or in combination, at a total MOI of 4, and ligand expression was assessed at both mRNA and cell surface expression level (Fig. 6). Statistical analysis of all AdV combinations for both ligands is reported in Table S1 and S2. Transduction efficiency of AdV-IE1 or AdV-IE2 was similar, with a percentage of IE+ cells on average of 61% and 68% at 3 dpi, respectively (data not shown).

Upon transduction, we observed a similar trend for modulation of both MICA mRNA and cell surface protein expression, with a significant up-regulation induced by IE2 compared to not-

transduced or AdV-LacZ-transduced cells, while IE1 did not affect MICA levels (Fig. 6A-B). Moreover, the combination of IE1 and IE2 expression did not induce a further increase in MICA mRNA and protein expression compared to IE2 alone (Fig. 6A-B and Table S1). When PVR was examined, its mRNA content was mostly up-regulated when both IE1 and IE2 were co-expressed, while IE1 or IE2 alone had no effect (Fig. 6C). Accordingly, PVR cell surface levels were mainly increased by the combined expression of the two proteins, while IE1 or IE2 alone induced only a modest increase of the ligand (Fig. 6D and Table S2).

Taken together, these results demonstrated that the virus-induced MICA and PVR up-regulation can be reproduced by the expression of the IE proteins only. However, their requirement is ligand-specific, since IE2 alone is sufficient to stimulate both MICA mRNA and protein expression, while co-expression of both IE1 and IE2 appear to be required for efficient PVR up-regulation.

Next, to examine the possibility that the up-regulation of MICA and PVR mRNA and cell surface levels induced by IE proteins involved the activation of ligand gene promoters, we performed transient transfection assays by co-transfecting HFFs with pGL3-MICA (containing a 1 kb fragment upstream from the *MICA* transcription start site) (Yadav D JI, 2009) or pGL2-PVR (-571 bp fragment) (Solecki D JBC 1997) luciferase reporter plasmids, together with expression vectors encoding the cDNAs of IE1 or IE2 proteins, used alone or in combination, or with the empty control vector pSG5 (Klucher MCB 1993). When the effect of IE1 and IE2, alone or in combination, was analyzed on the transcriptional activity of the *MICA* gene promoter, we observed that, while IE1 did not induce a significant modulation, IE2 was able to transactivate the promoter up to ~3-fold compared to the basal level obtained with the empty control vector

pSG5 (Fig. 7A). Co-transfection of IE2 with IE1 showed a further, though not significant, effect on *MICA* promoter activity, as compared to IE2 alone.

Since among the two major IE proteins, IE2 seemed to exert the major transactivating effect on the *MICA* gene promoter (Fig. 7A), we investigated further the mechanisms of this transcriptional regulation, by addressing both the IE2 structural requirements and the interaction with *MICA* gene promoter sequences. The IE2-55 protein is a splice variant of the IE2-86 gene product, with a conserved N-terminus and a 155 aminoacid deletion between residues 365 and 519 in the C-terminus. The region that is deleted has been shown to be required for many IE2-86 functions, including transcriptional activation and DNA binding (Malone et al., 1990, Pizzorno et al., 1991, Chiou et al., 1993, Schwartz 1994; Petrik and Stinski, 2008). Consequently, unlike IE2-86, IE2-55 fails to transactivate HCMV early promoters and to repress the Major IE Promoter (MIEP) (Klucher et al., 1993). Thus, we used an IE2-55 expression vector as a tool to investigate if the transcriptional activation and DNA binding properties of IE2-86, absent in IE2-55, were important to transactivate the *MICA* gene promoter. To this end, the co-transfection experiment with IE1 and IE2 proteins was performed replacing IE2-86 with IE2-55. Indeed, we observed that expression of IE2-55 completely abolished the activating effect of IE2-86 (Fig.7B), thus indicating that the C-terminus of IE2-86 is required for transactivation of *MICA* promoter. Moreover, it has been reported that a zinc finger mutant of IE2-86 cannot bind to the *cis*-repression signal in the MIEP (Jupp R JV 1993, due lavori). However, though this mutant cannot bind to DNA, it retains the ability to transactivate E gene promoters by protein-protein interactions (Jupp R JV 1993 67, 5595). We thus hypothesized that if the DNA binding ability of wild-type IE2-86 was important for *MICA* promoter activation, this should have been lost by substituting wild-type IE2-86 with its zinc finger mutant. Indeed, the co-transfection experiment

performed with IE1 and IE2-Zn mutant showed that the lack of the zinc finger hampered the ability of IE2-86 to transactivate *MICA* promoter (Fig. 7C). Together, these results indicated that the IE2 functional domains located primarily toward the C-terminal end of the protein are required for transactivation of the *MICA* gene promoter.

Next, to gain more insights into the molecular mechanisms behind the regulation of *MICA* promoter by IE proteins, we performed transient transfection assays with a shorter construct to map the region(s) targeted by the viral proteins. To this end, we tested the pGL3 MICA construct containing the luciferase gene driven by a 270 bp fragment upstream from the transcriptional start site of the *MICA* promoter region (MICA -270), together with the combination of IE1 and IE2, in light of the evidence that the effect of the two proteins did not significantly differ from the one mediated by IE1 alone (Fig. 7A). The shorter *MICA* fragment was indeed activated by IE1 and IE2 at similar levels compared to the longer *MICA* -1 kb region (Fig. 8A), indicating that the responsive region to IE proteins was contained within the 270 bp fragment.

The IE2-binding sites identified on different viral promoters, and on one cellular promoter as well, have been shown to contain invariant CG residues at both ends of a 10-nucleotide sequence (CG-N_{10}-CG), as reported in Fig. 8B (Waheed 1998;Lang, D. and Stamminger T JV 1993; Schwartz R. JV 1994; Arlt H JV 1994; Bresnahan WA, JBC 1998). A similar sequence, endowed of two CG residues separated by 10 internal nucleotides, is present within the *MICA* gene promoter, between residues –92 and –78, thus representing a potential IE2 binding site (Fig. 8B). To investigate the contribution of this putative IE-binding site to the overall IE2-dependent transactivation of *MICA* promoter, we changed by site-directed mutagenesis this unique CG-N_{10}-CG motif into a AT-N_{10}-AT sequence within the context of the pGL3 MICA (-270)

405 construct (Fig. 8B). As shown in Fig. 8A, the IE2-dependent transactivation of MICA was
406 significantly reduced by the introduced mutations, thus supporting an involvement of the
407 putative IE2-binding site in the IE2-mediated regulation of *MICA* gene promoter.
408 Next, to address the capability of IE1/IE2 proteins to directly bind to *MICA* promoter, we
409 performed Chip assays in highly transfectable 293T cells, in which pGL3-*MICA* (-270) was co-
410 transfected with the IE1 and IE2 expression vectors, or with the empty vector as a control.
411 Using an anti-IE antigen (anti-IE) antibody and specific primers to amplify the promoter region
412 containing the putative IE2 binding site, we observed that the viral IE1/IE2 proteins were
413 recruited to *MICA* promoter. The interaction was not detectable with the empty vector pSG5 or
414 using normal rabbit serum as a negative control (Fig. 8C). Finally, we performed the same
415 experiments by transfecting cells with wild-type or the CG mutant form of the *MICA* promoter,
416 and compared the relative DNA enrichment upon immunoprecipitation. As reported in Fig. 8D,
417 disruption of the putative IE2-binding site of the *MICA* promoter reduced IE binding of about
418 ~60%, further demonstrating that this sequence is involved in the IE2-dependent transactivation
419 of *MICA* promoter.
420 Together, these results demonstrated the capability of IE2 to directly bind sequences within
421 *MICA* gene promoter, and that this binding is required for MICA transcriptional activation.
422
423 In relation to PVR regulation, to evaluate the role of IE proteins on its transcriptional activation,
424 we performed similar transient co-transfection assays with the pGL2-PVR construct containing a
425 571 bp fragment upstream from *PVR* transcriptional start site (Solecki D, JBC 1997) and vectors
426 expressing IE proteins. IE1 had a relevant effect on *PVR* promoter, activating its transcription up
427 to 10-fold over the control (Fig. 9A). In contrast, IE2 alone was ineffective in stimulating *PVR*

promoter activity. However, the combination of IE1 and IE2 induced a prominent activation of the transcription that exceeded significantly that observed with IE1 alone (Fig. 9A). In contrast to what observed for *MICA*, IE2-55 and the IE2-86 zinc finger mutant did not affect the overall transactivation effect of the combination of IE1 and wild-type IE2-86 on *PVR* promoter activity (Fig. 9B-C), suggesting a different regulation of IE-mediated PVR up-modulation compared to what observed for MICA. Finally, we performed luciferase assays using progressive deletions of the promoter (Solecki JBC 1997), trying to identify the region(s) regulated by IE proteins, by transfecting both IE1 and IE2, as this was the more effective combination on *PVR* promoter (Fig. 9A). The results showed that we could identify a 213 bp fragment upstream from the transcriptional start site that was significantly less sensitive to IE proteins (Fig. 9C). The significant drop in luciferase activity observed with the deletion of sequences between -281 and -213 indicated that this fragment mediated most of the transactivating activity of IE1 and IE2 combination.

Taken together, the results included in this section indicate that the increase in cell surface expression of MICA and PVR upon HCMV infection is mediated by transcriptional events triggered by viral IE proteins.

Discussion

The molecular mechanisms driving the expression of NKG2D and DNAM-1 ligands remain largely unknown and, in particular, very little is known concerning the mechanisms of their induction in virus-infected cells. In this study, we have investigated the impact of HCMV infection on the expression of NKG2D and DNAM-1 ligands, under a different perspective compared to most of the work performed so far by many investigators, including us. In fact, the majority of the studies on NK/T cell activating ligands in HCMV-infected cells have been focused on the mechanisms evolved by the virus to escape recognition by cytotoxic lymphocytes. The HCMV genome is indeed often described as a paradigm of viral immune evasion, with several genes dedicated at eluding immune defenses (ref), including at down-modulating both NKG2D and DNAM-1 ligands (ref). On the other hand, it seems likely that NKG2D evolved and has been conserved to provide immunity against pathogens, and the redundancy of its ligands and their extensive allelic polymorphism might be driven by selective pressures of those pathogens that are evolving mechanisms to escape detection by immune cells using NKG2D (ref). More recently, also DNAM-1 has been shown to be important in anti-viral immunity (ref), including murine and human CMV infection (ref). Therefore, novel therapeutic strategies to restore or enhance NKG2D- and DNAM-1-dependent activation of NK or T cells may be beneficial at harnessing their anti-viral activity, and a better understanding of the mechanisms regulating NKG2D and DNAM-1 ligand expression in infected cells is needed.

The results shown here demonstrated that, in most of the cell type-viral strain combinations we investigated, MICA, ULBP3 and PVR ligands were up-regulated on the plasma membrane of infected cells. In particular, we observed an increased MICA expression on infected HFFs, independently from the strain used, while infection of endothelial or epithelial cells with low-

468 passage strains resulted in no up-regulation or down-regulation of cell surface levels,
469 suggesting that increased or *de novo* MICA expression may be restricted to certain cell types.
470 However, the evidence that MICA was induced on HFFs by both laboratory and low-passage
471 strains, suggests that the down-modulating activity exerted on MICA by UL142, US18 and US20
472 viral gene products (Chalupny NJ BBRC 2006; Ashiru O JV 2009; Fielding 2014) was not
473 adequate to prevent its cell surface expression. Of note, UL142 has been described to prevent
474 cell surface expression of ULBP3 as well (Bennett NJ JI 2010), but in our settings its expression
475 was always increased, independently from the cell type, the viral strain and the amount of virus
476 employed, consistent with previous findings (Rolle JI 2003). The discrepancies may be related
477 to different experimental settings, as well as to different cells and viruses employed. In fact, a
478 considerable polymorphism exists in the UL142 sequence among different strains, including
479 amino acid insertions (Chalupny NJ BBRC 2006), and it is thus possible that some variants of
480 UL142, US18 and/or US20 are less efficient at down-modulating MICA and ULBP3 expression
481 than others. At the same time, polymorphisms in both the coding and non-coding regions of
482 MICA and ULBP3 have been described, and this may also modulate NKG2D ligand expression
483 upon HCMV infection.
484 At present, there are few reports on PVR expression upon HCMV infection of fibroblasts and
485 myeloid dendritic cells (Tomasec P, Nature Immunol 2005, Prod'homme V, JGV 2010, Magri G,
486 Blood 2011). In relation to fibroblasts, despite it was shown that PVR was down-modulated by
487 the low-passage strain Merlin, we instead consistently and reproducibly observed a significant
488 up-regulation of cell surface PVR with both low-passage and laboratory strains, under all
489 experimental conditions tested. PVR was also up-regulated at the mRNA level in AD169-
490 infected HFFs. Though the discrepancies could be due to different experimental settings (e.g.,

MOI 1 instead of MOI 25; use of fibroblasts, as well as of epithelial and endothelial cells), our results show for the first time that PVR can be upregulated upon HCMV infection, in different cell types and with different viral strains, offering the immune system the opportunity to detect and react against infected cells through the activating receptor DNAM-1. In fact, this receptor has been suggested to play a relevant role in NK cell recognition of HCMV-infected myeloid dendritic cells early during infection, whereas the effect of viral-mediated down-regulation of DNAM-1 ligands prevails at later stages, thus also illustrating the importance of the kinetics of immune evasion mechanisms (Magri G, Blood 2011). DNAM-1 is remarkable as it is expressed by all NK cells and is an important activator of their effector functions (Martinet Immunol Cell Biol 2014). However, the increased PVR expression caused by HMCV infection may have ramifications that extend beyond the regulation of NK cell functions, as DNAM-1 is also expressed by a big variety of leukocytes (activated T cells, NKT cells, a B cell subset, myeloid cells, mast cells, megakaryocytes and platelets), thereby impacting on a wide range of immunological responses (Bachelet., 2006; Bottino., 2003; Burns, 1985; Pende., 2006; Reymond, 2004; Scott, 1989; Shibuya, 1996, 1999, 2003; Xu & Jin, 2010; Tahara-Hanaoka 2004; Takai 2008; Martinet Immunol Cell Biol 2014). In addition, PVR expression may impact anti-viral immune responses mediated by two other receptors engaged by this ligand, Tactile (CD96) (Fuchs JI 2004) and TIGIT (Staniesky N PNAS 2009).

To gain insights into the molecular mechanisms regulating activating ligand expression in infected cells, we investigated the role of DDR, a pathway positively affecting the expression of these molecules (Cerboni Rev Frontiers 2014) and activated by HCMV (Castillo JV 2005). We observed an HCMV-induced DDR activation, as revealed by the increased histone H2AX phosphorylation, but MICA, ULBP3 and PVR were still up-modulated in HCMV-infected HFFs in

514 which ATM, ATR, and/or DNA-PK were knocked-down, thus indicating that these kinases do not
515 play a role in activating ligand up-regulation in HCMV-infected cell, similarly to what has been
516 reported for murine NKG2D ligands in MCMV infection (Tokuyama Plos Pathogens 2011).
517 The observation that activating ligands were still expressed upon treatment of infected cells with
518 the viral inhibitor phosphonophormic acid suggested that viral IE proteins – which are
519 insensitive to inhibitors of viral DNA synthesis - were involved in these regulatory mechanisms.
520 HCMV IE proteins have been previously suggested to be implicated in the transcriptional
521 activation of MIC genes (Venkataraman, Andresen JI 2007), but several pieces of the puzzle
522 were missing, including the effect of the single versus the combination of the two IE, the
523 molecular mechanism(s) of such regulation, and the promoter region eventually responsive to
524 viral IE. In relation to PVR, no data have been instead reported on its HCMV-induced increase
525 and on the molecular mechanism(s) involved. Our results show that ectopic expression of IE1
526 and IE2 induced a significant increase of MICA and PVR, both at the mRNA and cell surface
527 expression level. In particular, IE2 emerged as the main transactivator of MICA promoter, with
528 the effect strictly dependent on its DNA binding activity, as it was lost in the presence of the IE2-
529 55 isoform and of the zinc finger mutant form of IE2-86. Accordingly, by ChIP and mutagenesis
530 approaches, we identified an IE2 consensus sequence in MICA promoter, critical for its
531 activation by this viral protein. Our study contributes to challenge the prevailing view that
532 activation of cellular genes by IE2 is due to protein-protein interactions. In fact, it was initially
533 thought that IE2 activates cellular promoters by interacting with basal transcription factors,
534 raising the notion that nucleotide-specific binding of IE2 to cellular promoters did not occur,
535 despite this appeared to be the predominant mode of regulation of HCMV promoters. However,
536 in 1998 Bresnahan and co-workers demonstrated that IE2 was capable to activate the cyclin E

promoter via a DNA-binding mechanism. In addition, they noticed that the IE2-binding sites within the cyclin E promoter differed from those observed within HCMV promoters, with the 10-internal nucleotides of the CG-N_{10}-CG motifs being GC-rich, rather than AT-rich (ref). Similarly, the MICA IE2-binding site we have identified appears to be GC-rich, further supporting the idea that IE2 is relatively sequence tolerant. It is also possible that IE2 DNA binding ability to cellular promoters relies more on GC-rich than AT-rich motifs. However, since the cellular promoters described so far to which IE2 directly binds are only two (cyclin E and MICA), this aspect needs further investigations. Moreover, this is the first evidence that IE2 binds to and activates a promoter of a cellular gene involved in the elimination of infected cells by cytotoxic lymphocytes, and opens the possibility that other viruses may use their encoded proteins to directly induce activating ligand expression.

In relation to PVR, our results demonstrate a different mechanism of its up-regulation. PVR mRNA and protein expression were mostly increased by the co-expression of IE1 and IE2, an observation further confirmed in transfection assays, in which IE1 was able to significantly transactivate the promoter, but with a maximal activation obtained by the combination of the two IE proteins. Experiments performed using progressive deletions of PVR promoter allowed us the identification of a region between -281 bp and -213 bp mediating most of the transactivation activity of IE1/IE2 combination. Though this fragment contains a potential IE2-responsive CG-N_{10}-CG element (from -271 to -257: CG-CAGGCGCAGG-CG), direct DNA binding of IE1/IE2 proteins to PVR promoter does not occur, since i) the IE2-55 isoform and the zinc finger mutant of IE2 retained the capability to activate PVR promoter, and ii) IE1 seems not to bind DNA directly (Castillo and Kowalik 2002). Thus, a possible mechanism of PVR regulation is that in the -281/-213 bp region could map the binding site(s) of other factor(s) recruited and/or

activated by IE proteins. However, PVR promoter regulation is largely unknown and further investigations are needed to identify its transactivator(s).

One question that could arise is why a virus should increase the expression of molecules involved in the elimination of infected cells. One possibility is that this could be a side effect of the strong transactivating activity of HCMV IE proteins, and in particular of IE2. In fact, this protein is crucial for a productive viral replication, so that the virus cannot avoid to express IE2 to survive (Castillo 2002). Moreover, it could be related to MICA gene polymorphism. In fact, many different MICA genetic variants exist, with polymorphisms described both in the promoter and coding regions. Of note, the IE2-consensus sequence we identified is conserved among different allelic variants of MICA promoter (our unpublished observations and Cox ST Tissue Antigens 2014; Jia Luo Human Immunol 2014). These observations suggest that, during the virus-host coevolution, a positive selection of promoter sequences in MICA alleles carrying the IE2 DNA binding site occurred, and that the host has made IE2 useful for its cellular gene expression as well.

However, how can we reconcile the observed increase in the expression levels of MICA, ULBP3 and PVR upon HCMV infection, with the immunoevading strategies evolved by the virus to target activating ligands? Our results suggest that there could be a temporal window in the early phases of the infection, during which the expression of NKG2D and DNAM-1 ligands induced by IE proteins precedes the expression of virus-encoded immunoevasion proteins. In this *window of opportunity*, with elevated, functionally relevant levels of activating signals, the immune surveillance against the viral infection could be sufficiently robust, allowing recognition of infected cells by cytotoxic lymphocytes. Another option could be linked to tissue compartmentalization of HCMV in human hosts. A hallmark of HCMV infections is dissemination

583 to a wide range of host tissues and cell types (Sinzger JV 1995,) and quantitative descriptions
584 of the virus have pointed out significant differences in the level of diversity between
585 compartments, e.g., with blood populations appearing more diverse than urine or intraocular
586 populations (Sowmya P J Med Virol 2009; Renzette N Plos Genetics 2013; Renzette N Curr
587 Opin Virol 2014). Although it is not clear yet neither the mechanism explaining HCMV
588 compartmentalization and intrahost genetic diversity nor their effects on clinical disease, one
589 possibility is that the generation of mutants may influence NK cell and/or T cell recognition,
590 depending on the compartment (Renzette N Curr Opin Virol 2014). Therefore, the balance
591 between expression and down-modulation of NK/T cell activating ligands, and thus between
592 immunorecognition and immunoevasion, may vary depending also on HMCV diversity and
593 tropism. We thus believe that a better understanding of the cell-intrinsic and -extrinsic
594 mechanisms regulating NKG2D and DNAM-1 ligands, and consequently affecting immune
595 responses mediated by these activating receptors expressed by cytotoxic lymphocytes is
596 needed to take full advantage of this potent immune pathway.
597

Materials and methods

Antibodies and reagents

The following monoclonal antibodies (mAbs) were used in flow cytometry: anti-MICA (M673) and anti-ULBP4 (M475) from Amgen (Seattle, USA); anti-MICA (AMO-1) from BamOmaB (Axxora, Gräfelfing, Germany); anti-MICB (MAB236511), anti-ULBP1 (MAB170818), anti-ULBP2 (MAB165903), and anti-ULBP3 (MAB166510) from R&D Systems (Minneapolis, MN); anti-Nectin-2 (CD112) from BD Biosciences (San Diego, CA); anti-PVR (SKII.4) kindly provided by Dr M. Colonna (Washington University, St Louis, MO); Alexa fluor 488-conjugated anti-IE antigens (MAB810X) and FITC-conjugated anti-phospho-histone H2AX (γH2AX) (Ser139; clone JBW301) from Merck Millipore (Darmstadt, Germany); mouse control IgG1 from Biolegend (San Diego, CA); goat anti-mouse (GAM)-APC from Jackson Immunoresearch Laboratories (West Grove, PA); GAM-FITC from Cappel (Milan, Italy); mouse control IgG_1-FITC from BD Biosciences (San Diego, CA). The following antibodies were used in immunoblotting: anti-p85 subunit of PI-3 kinase from Merck Millipore (Darmstadt, Germany); anti-ATM (D2E2) from Cell Signaling Technology (Danvers MA); anti-ATR (sc-1887) and anti-DNA-PK_{CS} (sc-5282) from Santa Cruz (Dallas, TX).

Other reagents used were: gelatin, caffeine, methylcellulose, NU7026, phosphonoformic acid (PFA) (Foscarnet) and crystal violet from Sigma Aldirch (St. Louis, MO); Lipofectamine 2000 from Invitrogen (Thermo Fisher Scientific, Waltham, MA), Dharmafect from Dharmacon (GE Healthcare, Buckinghamshire, UK).

Cells and culture conditions

Primary human foreskin fibroblasts (HFF), the retinal epithelial cell line ARPE-19 and the human embryo kidney 293T cells were purchased from the American Type Culture Collection (ATCC). HFF and 293T cells were grown in Dulbecco's modified Eagle medium (DMEM) containing 10% fetal calf serum (FCS), 2 mM glutamine, 1 mM sodium pyruvate, 100 U/ml penicillin, and 100 μg/ml streptomycin sulfate, and ARPE-19 cells in a 1:1 mixture of DMEM and Ham's F-12 medium (Invitrogen) containing 10% FCS, 15 mM HEPES, 2 mM glutamine, 1 mM sodium pyruvate, 100 U/ml penicillin, and 100 μg/ml streptomycin sulfate. HFFs were used at passages 14 to 28. Human dermal microvascular endothelial cells (HMVECs) (CC-2543) were obtained from Clonetics (San Diego, CA) and cultured in endothelial growth medium (EGM) corresponding to endothelial basal medium (EBM) (Clonetics), containing 10% FCS, human recombinant vascular endothelial growth factor (VEGF), basic fibroblast growth factor (bFGF), human epidermal growth factor (hEGF), insulin growth factor 1 (IGF-1), hydrocortisone, ascorbic acid, and heparin. Cells were seeded onto culture dishes coated with 0.2% gelatin. Experiments were carried out with cells at passages 4 to 15. Fibroblasts derived from an Ataxia Telangectasia Mutated patient and not expressing ATM protein (AT-/-), were kindly provided by Drs. M. Fanciulli and T. Bruno (Regina Elena National Cancer Institute, Rome, Italy). They were grown in DMEM containing 15% FCS and used at passages 5 to 8. All cells were maintained at 37°C in a 5% CO_2 atmosphere.

HCMV preparations and infection conditions

The HCMV AD169 strain (ATCC-VR538), was prepared by infecting semi-confluent layers of HFF cells at a virus-to-cell ratio of 0.01, and cultured until a marked cytopatic effect was seen. Stocks were then prepared after 3 rounds of cell freezing and thawing, subjected to centrifugal

clarification, and frozen at −80°C. Virus titers were measured by standard plaque assays on HFF cells. Stock solutions used in all experiments contained approximately $2x10^7$ PFU/ml. Standard plaque assays were used also in different experiments to determine viral titers in the supernatants harvested from infected cells.

HCMV TR was derived from an ocular specimen (Smith IL, Arch Ophthalmol 1998), and after a few passages on fibroblasts, was cloned into a BAC (Murphy E PNAS 2003; Ryckman BJ JV 2006). Reconstitution of TR BAC in fibroblasts was performed as previoulsy described (Bronzini et al., J Virol 2012) by co-transfecting HFFs with the corresponding TR BAC and a plasmid expressing HCMV pp71. Reconstituted infectious virus retained the ability to infect endothelial and epithelial cells, as well as monocytes and macrophages (Ryckman BJ JV 2006; Bronzini et al., 2012). HCMV VR1814 is a derivative of a clinical isolate recovered from a cervical swab of a pregnant woman (Revello JGV 2001). This strain was propagated in HUVEC and titrated as previously described (Caposio P, Antiviral Res 2007).

Cells were infected at about 80-90% confluence at a multiplicity of infection (MOI) of 1 PFU/cell, unless otherwise specified, in their respective culture medium, without FCS. Virus adsorption was carried out for 2 h (AD169, or TR) or 5 h (VR-1814) at 37°C, and the virus inoculum was then discarded and replaced with fresh growth medium (day 0). Mock-infected control cultures were exposed for the same amount of time to an equal volume of mock-infecting medium. At various days post-infection (dpi), cells were harvested and analyzed. In some experiments, phosphonoformic acid (PFA) was added after virus inoculation at a final concentration of 200 µg/ml, while caffeine was added 2 dpi at a final concentration of 10 mM.

Adenovirus vectors and infections

667 Recombinant adenoviruses (AdV) encoding HCMV IE86 (AdV-IE86) and *E. coli* β-galactosidase
668 (AdV-LacZ) have been previously described (Gariano et al., Plos Path 2012; Mercorelli B et al.,
669 AAC 2014), while AdV-IE72 was kindly provided by Dr. Timothy F. Kowalik (University of
670 Massachusetts Medical School, Worcester, USA) (Wilkinson, GW, and A. Akrigg. 1992. Nucleic
671 Acids Res.; Ahn, JH., and GS Hayward. 1997. J. Virol; Castillo, JP, AD Yurochko, and TF
672 Kowalik. 2000. J. Virol). Recombinant AdV stocks were generated, purified and titrated as
673 previously described (Gariano et al., Plos Path 2012; Mercorelli et al., AAC 2014; Castillo, JP,
674 AD Yurochko, and TF Kowalik. 2000. J. Virol).
675 For adenoviral transduction, HFFs were infected at about 80-90% confluence at an MOI of 4
676 pfu/cell in DMEM without FCS, for 2 h at 37°C. When the viral proteins were not expressed in
677 combination, the total MOI was equalized to 4 with AdV-LacZ. After 2 h, the virus inoculum was
678 discarded and replaced with fresh growth medium (day 0) and analyzed at the indicated dpi.
679 Mock-infected cells served as control cultures. Following infection, cultures were maintained in
680 growth medium and analyzed at the indicated dpi.
681
682 **Immunofluorescence and FACS analysis**
683 Mock-infected or infected cells were harvested at the indicated dpi and stained with mAbs
684 specific for MICA, MICB, ULBP1-4, PVR and Nectin-2, followed by GAM-APC or by GAM-FITC
685 (for experiments with PFA), and analyzed by flow cytometry on an FACSCalibur (Becton
686 Dickinson). The mean of fluorescence intensity (MFI) value of the isotype control antibody was
687 always subtracted from the MFI relative to each molecule. For intracellular staining of IE
688 antigens or phosho-histone H2AX (γH2AX), cells were fixed in 1% formaldehyde, permeabilized
689 with 70% ethanol, and then incubated with Alexa fluor 488-conjugated anti-IE mAb (MAB810X)

690 or with FITC-conjugated anti-γH2AX (JBW301), respectively.

691

692 **Immunoblot analysis**

693 Cells were lysed for 20 minutes at 4°C in a lysis buffer containing 0.2% Triton X-100, 0.3%
694 NP40, 1 mM EDTA, 50 mM Tris HCl pH 7.6, 150 mM NaCl, and protease inhibitors to obtain
695 whole-cell protein extracts.. Protein concentration was measured with the Bio-Rad Protein
696 Assay. Lysates (30-40 μg) were resolved by SDS-PAGE and transferred to nitrocellulose
697 membranes (Merck Millipore). Membranes were blocked with 5% milk and probed with the
698 indicated antibodies. Immunoreactivity was revealed using an enhanced chemiluminescence kit
699 (Amersham).

700

701 **siRNA**

702 The ON-TARGETplus SMARTpool siRNA specific for ATM and ATR (siATM, siATR), and the
703 ON-TARGETplus non-targeting pool (siCtrl) were purchased from Dharmacon (Thermo Fisher
704 Scientific). siRNA specific for DNA-PK$_{CS}$ (sc-35200) (siDNA-PK) was from Santa Cruz. HFF
705 cells (70%-80% confluence) were transfected with 100-200 nM of siRNA using DharmaFECT
706 siRNA Transfection Reagent (Thermo Fisher Scientific), according to the manufacturer's
707 recommendations. One to two days after transfection, cells were infected with AD169, as
708 indicated in the figure legends. Cells and supernatants were harvested and analyzed at 2 or 3
709 dpi, as indicated.

710

711 **RNA isolation and real-time PCR**

712 Total RNA was extracted using TRI Reagent Solution (Life Technologies Inc., Grand Island,

NY), according to manufacturer's instructions, and 1 μg of total RNA was used for cDNA first-strand synthesis in a reaction volume of 25 μl. Real-Time PCR was performed using the ABI Prism 7900 Sequence Detection system (Applied Biosystems, Foster City, CA); cDNAs were amplified in triplicate with primers for MICA (Hs00792195_m1), PVR (Hs00197846_m1), and GAPDH (Hs03929097_g1), using specific TaqMan Gene Expression Assays (Applied Biosystems, Foster City, CA). Relative expression of each gene versus GAPDH was calculated according to the $2^{-\Delta\Delta Ct}$ method.

Plasmids

The pGL3-*MICA* promoter vector was previously described (Yadav DJ et al, JI 2009) and kindly provided by Dr. J. Bui (University of California at San Diego, La Jolla, CA). To generate the *MICA* -270 promoter plasmid, a fragment of 270 bp was obtained by cutting the 3.2 WT GFP reporter (Dr. Skov, University of Copenhagen, Denmark) with the enzymes *KpnI* and *BglII*, and cloned in pGL3-Basic luciferase vector (Promega Corp., Madison, WI) (Soriani JI 2014). Mutant *MICA* -270-CG construct was generated using Quick Change Site-Directed Mutagenesis Kit (Stratagene, La Jolla, CA) following the manufacturer's instructions. Primers were designed to generate two CG mutations in the *MICA* promoter region of the pGL3 -270 bp *MICA*. Primer sequences used were: -92 bp **-CG**GTCGGGGGAC**CG** -78 bp; primers for mutagenesis: forward 5' -CCAGTTTCATTGGATGAGATGTCGGGGGACATGGCCAGGTGACTAAG-3'; reverse 5'-CTTAGTCACCTGGCCATGTCCCCCGACATCTCATCCAATGAAACTGG-3'. Inserted mutations were verified by sequencing.

734 The pGL2-Basic luciferase vector containing -571 bp of the human *PVR* promoter and
735 progressive deletions (-470 bp, -343 bp, -281 bp and -213 bp) were kindly provided by Dr. G.
736 Bernhardt (Hannover Medical School, Hannover, Germany) (Solecki et al., 1997).
737 pSG5-IE72, pSG5-IE86, and pSG5-IE55 constructs contained the full-length cDNAs of the viral
738 IE proteins, cloned in the pSG5 vector (Stratagene) (Klucher et al., 1993). The IE86 cDNA
739 cloned in the pRSV vector, and the zinc finger mutant of IE86, with cysteines 428 and 434
740 mutated into serine residues (pRSV-IE86-Zn mut), were a generous gift of Prof. Jay Nelson and
741 were previously described (Jupp R et al, JV 1993).
742
743 **Transfection and luciferase assay**
744 In all transfection experiments, 3 µg of luciferase reporter, 0.25 µg of pRL-CMV-Renilla, and 2
745 µg of IE protein vectors or of pSG5 empty vector were co-transfected into 80-90% confluent
746 cells growing on a 10 cm^2 area using Lipofectamine 2000 (Invitrogen) according to the
747 manufacturer's protocols. In some experiments, the pSG5-IE86 vector was replaced by pSG5-
748 IE55, pRSV-IE86 or pRSV-IE86-Zn-mut, as indicated. 48 hours post-transfection, cells were
749 harvested and prepared for the luciferase assays, using the Dual-Luciferase Reporter Assay kit
750 and the Glomax Multi Detection System (Promega Corp., Madison, WI) following the
751 manufacturer's instructions. Relative luciferase activity was calculated by dividing the luciferase
752 activity of pGL3-MICA or pGL2-PVR reporter, co-transfected with pSG5, by the respective
753 pGL3- or pGL2-Basic, to remove the unspecific effect of IE proteins on the reporter vector. The
754 unspecific modulation of the reporter empty vector activity was probably due to a general
755 activation of the transcriptional machinery by IE proteins, and was more evident for IE1. A
756 similar correction allowed us to better appreciate the specific effect of the viral proteins on

ligand promoters.

Chromatin immunoprecipitation assay (ChIP)

293T cells were co-transfected with 5 µg of *MICA* -270 promoter plasmid, wild-type or mutated, and pSG5-IE72 (10 µg) and pSG5-IE86 (10 µg), or pSG5 empty vector (20 µg), using Lipofectamine 2000. After 48 hours, cells were cross-linked, harvested, and processed for ChIP assays following the manufacturer's protocol of Magna ChIP AG chromatin immunoprecipitation kit (Merck Millipore). Nuclei were isolated and chromatin was sonicated to generate 150-300 bp fragments. Samples were immunoprecipitated overnight with 20 µl of a polyclonal rabbit anti-IE antibody, that we generated and recognizing from 1 to 429 aa of HCMV IE2-86 protein, or with an equivalent amount of a polyclonal rabbit serum used as control, and 20 µl of protein AG magnetic beads. Immunoprecipitates were washed and digested with proteinase K for 2 hours at 62°C. DNA was purified using spin columns and eluted in 50 µl of eluting reagent. 20 µl of pre-cleared chromatin were processed as immunoprecipitated chromatin, for input DNA controls. Purified DNA was quantified by real-time PCR, using the Power-SYBR Green mix (Applied Biosystems, Foster City, CA). Primer sequences used were: MICA promoter forward 5′-AGGTCTCCAGCCCACTGGAATTTTCTC-3′; MICA promoter reverse 5′-CGCCACCCTCTCAGCGGCTCAAGC-3′. PCRs were validated by the presence of a single peak in the melt curve analysis, and amplification of a single specific product was further confirmed by electrophoresis on agarose gel. Results are expressed as relative enrichment as compared to the input. Negative control (polyclonal rabbit serum) values were subtracted from the corresponding samples. Absolute quantifications were obtained by serial dilutions of the

779 input DNA samples. The analysis was performed using the SDS version 2.4 software (Applied
780 Biosystems).
781
782 **Confocal microscopy analysis**
783 For staining of cell surface MICA, HFFs were grown to semi-confluence on glass coverslips in
784 24-well plates and infected with AD169 and TR at a MOI of 1 PFU/cell for 2 h at 37°C. After 4
785 dpi, cells were washed with PBS, fixed in 1% paraformaldehyde for 15 min at room-temperature
786 (RT), blocked in 1% FCS diluted in PBS (20 min., RT), but not permeabilized, to not allow mAb
787 entry into the cells. Indirect immunofluorescence analysis was performed by incubating fixed
788 cells with the anti-MICA mAb AMO-1 (1:40) for 2 h at 37°C, followed by secondary antibody
789 incubation with CF594-conjugated rabbit anti-mouse IgG (Sigma) for 1 h at RT. Samples were
790 then visualized with an Olympus IX70 inverted laser scanning confocal microscope, and images
791 were captured using FluoView 300 software (Olympus Biosytems).
792
793 **Statistical analysis**
794 Statistical analysis of the data was performed using a paired Student *t*-test. A value of $p<0.05$
795 was considered statistically significant.
796

Figure legends

Figure 1. Evaluation of NKG2D and DNAM-1 ligand expression on AD169-infected fibroblasts. HFFs were infected with the HCMV laboratory strain AD169 (black line) at an MOI of 1 PFU/cell or mock-infected (n.i., grey filled histograms) and harvested at different days post-infection (dpi), as indicated. Ligand expression was evaluated by FACS analysis on cells stained with mAbs specific for MICA, MICB, ULBP1-4, PVR and Nectin-2, followed by GAM-APC. **A)** A representative experiment of at least four performed at 3 dpi is shown. Dashed lines indicate mock-infected (n.i.) or infected cells stained with isotypic control IgG. **B)** The kinetics of ligands with an increased expression upon HCMV infection is shown. Expression levels are presented as mean of fluorescence intensity (MFI). MFI of isotypic control IgG was subtracted from the MFI relative to each ligand. Values represent the mean of at least four independent experiments ± standard error (SE). * $p<0.05$; ** $p<0.01$; ** $p<0.001$ with Student's *t*-test of n.i. versus HCMV-infected cells.

Figure 2. NKG2D and DNAM-1 ligands are up-regulated on different cell types by HCMV low-passage strains VR-1814 and TR. HFFs, HMVECs or ARPE-19 cells were not infected (n.i.) or infected with the indicated HCMV low-passage strain. Cells were then harvested at 3 dpi and ligand expression was evaluated by FACS analysis with mAbs specific for MICA, ULBP3 and PVR, or with an isotype control IgG, followed by GAM-APC. **A)** A representative experiment of HFFs infected with the low-passage strain VR-1814, and with AD169 as a control, is shown. **B)** HFFs were infected with VR-1814 at MOI of 1 and 5 PFU/cell, and the expression of MICA, ULBP3, and PVR was assessed at 3 dpi. Expression levels are presented as the mean of three

independent experiments ± SE. **C)** HFFs, HMVECs, and ARPE-19 were infected with TR or VR-1814 at a MOI of 1 PFU/cell and the expression of MICA, ULBP3, and PVR was measured at 3 dpi. Expression levels are presented as the mean of at least three independent experiments ± SE. In panels B) and C) expression levels are presented as mean of fluorescence intensity (MFI), calculated as in figure 1. * $p<0.05$; ** $p<0.01$ with Student's *t*-test of n.i. versus HCMV-infected cells. The percentage of infected cells (measured by intracellular staining with the anti-IE mAb) was as follows: HFF with VR1814 (MOI 1): 45±10%; HFF with TR: 96±0%; HMVEC with TR: 76±8%; HMVEC with VR1814: 44±11%; ARPE-19 with TR: 77±6%; ARPE-19 with VR1814: 48±6%.

Figure 3. Triple silencing of ATM, ATR and DNA-PK does not affect MICA, ULBP3 and PVR expression. HFF were firstly transfected with siDNA-PK or with siCtrl. 24 h later, the same cells were co-transfected with siATM and siATR, or with siCtrl. 24 h later, cells were either uninfected or infected with HCMV (AD169) at MOI 1 PFU/cell, then, at 3 dpi cells and supernatants were harvested and assayed for ligand expression, immunoblot analysis, percentage of IE+ cells, and infectious virus production. **A)** Flow cytometry analysis of MICA, ULBP3 and PVR expression, as described in figure 1. Vertical dotted lines indicate the center of the peak for each ligand in not infected-siCtrl transfected cells. All panels derive from the same experiment, representative of three. **B**) The levels of ATM, ATR and DNA-PK protein expression were assayed by immunoblot analysis with antibodies specific for each molecule. p85 subunit of PI-3K was used as a control of protein loading. **C)** The % of IE+ cells was analyzed by flow cytometry on HCMV-infected cells by intracellular staining with a specific anti-IE mAb. **D)** Cell culture supernatants were assayed for infectious virus production by plaque assay. ns: not

statistically significant difference with Student's t-test. siDDR: cells transfected with siATM, siATR and siDNA-PK.

Figure 4. Immediate early and early genes, but not late genes, are *per se* sufficient to increase the expression of MICA, ULBP3 and PVR in infected cells. HFFs were infected with HCMV AD169 (MOI of 1 PFU/cell) or mock-infected, and then treated with 200 μg/ml of phoshonoformic acid (PFA) immediately after infection. At 3 dpi, cells were harvested and stained for MICA, ULBP3, PVR or isotype control IgG, followed by GAM-FITC. One representative experiment out of three is shown.

Figure 5. Up-regulation of MICA and PVR mRNA in HCMV-infected cells. HFFs cells were infected with HCMV AD169 at an MOI of 1 PFU/cell or mock-infected. At the indicated times post-infection, total RNA was purified and reverse transcribed. cDNAs were amplified by real-time PCR using primers specific for MICA, PVR, or GAPDH. Data, expressed as fold change units, were normalized with GAPDH and referred to not infected cells considered as calibrators, and set at 1. Values represent the mean of two independent experiments ± SE.

Figure 6. Adenoviral-mediated overexpression of IE1 and IE2 proteins increases mRNA and cell surface expression of MICA and PVR. HFFs were transduced with adenoviral vectors (AdV) expressing IE1, IE2, or LacZ uas a control, alone or in combination, at a total MOI of 4 PFU/cell. Cells were harvested at 48 h (for mRNA) or at 72 h (for cell surface expression) post-transduction, and analyzed for ligand mRNA content and surface expression, respectively. **A) and C)** Real-time PCR was performed with primers specific for MICA **(A)** and PVR **(C).** Data,

866 expressed as fold change units ± SE**,** were normalized with GAPDH and referred to not-
867 transduced cells (-), considered as calibrators and set at 1. Values derive from four independent
868 experiments. **B) and D)** Cell surface expression levels of MICA **(B)** and PVR **(D)** as measured
869 by FACS are presented as mean of fluorescence intensity (MFI), as described in figure 1.
870 Values represent the mean of three independent experiments ± SE. ns: not significant; *
871 $p<0.05$; ** $p<0.01$; *** $p<0.001$ with Student's t-test. See Tables S1 and S2 for a complete
872 statistical analysis.
873
874 **Figure 7. IE2 activates *MICA* promoter: role of IE2 DNA binding activity. A)** HFFs were
875 transiently transfected with pGL3-MICA (-1 Kb fragment) luciferase reporter plasmid, together
876 with expression vectors containing the cDNA of the indicated IE proteins, used alone or in
877 combination, or with the empty control vector pSG5. After 48 h, transfected cells were harvested
878 and protein extracts were used for luciferase assay. Luciferase activity was calculated as
879 described in Materials and Methods, and results are expressed as fold-induction compared to
880 the empty control vector. **B) and C)** IE2-86 was replaced by IE2-55 **(B)** or by a zinc finger
881 domain mutant IE2-86 (IE86 Zn mut) **(C)**. IE2-86 Zn mut was cloned into pRSV vector, so in
882 panel C pRSV and pRSV-IE2-86 were used as controls. Data represent the mean value from at
883 least three independent experiments ± SE. ns: not significant; * $p<0.05$; ** $p<0.01$ with Student's
884 t-test.
885
886 **Figure 8. Identification of an IE2 consensus site in *MICA* promoter. A)** HFFs were
887 transiently transfected with wild-type (wt) pGL3-*MICA* (-270 bp fragment) promoter luciferase
888 reporter vector, or with a mutated form (CG-mut), together with plasmid vectors containing the

889 cDNA of IE1 and IE2, or with the empty control vector pSG5. After 48 h, cells were harvested
890 and luciferase activity was calculated as described in figure 7. Data represent the mean values
891 from three independent experiments ± SE. **B)** the CG-N_{10}-CG sequence identified on MICA
892 promoter, and its mutated form (CG-mut), are reported and compared with some of the IE2-
893 binding sites described on the HCMV MIEP, the 2.2 Kb early promoter and the cyclin E
894 promoter. **C)** 293T cells were co-transfected with wt pGL3-*MICA* (-270 bp fragment) promoter,
895 and plasmid vectors containing IE1 and IE2 cDNAs, or with pSG5. After 48 h, cells were
896 harvested and processed for the ChIP assay, as described in material and methods. Results
897 are shown as relative enrichment of samples immunoprecipitated with the anti-IE antibody (anti-
898 IE) in respect to IgG control. Data represent the mean values from three independent
899 experiments ± SE. **D)** Both the wt and the mutant form of -270 bp *MICA* promoter were used in
900 ChIP experiments, and the relative enrichment was compared. Data are expressed as percent
901 of IE binding, with the relative enrichment of MICA -270 wt promoter set as 100%. Data
902 represent the mean value from three independent experiments ± SE. * $p<0.05$; ** $p<0.01$; ***
903 $p<0.001$. MIEP: major immediate early promoter.
904
905 **Figure 9. Effect of IE1 and IE2 on the transcriptional activity of *PVR* gene promoter. A)**
906 HFFs were transiently transfected with pGL2-PVR (-571 bp fragment) promoter luciferase
907 reporter vector, together with plasmid vectors containing the cDNA of the indicated IE proteins,
908 used alone or in combination, or with the empty control vector pSG5. After 48 h, cells were
909 harvested and luciferase activity was calculated as reported in figure 7. **B) and C)** IE2-86 was
910 replaced by IE2-55 **(B)** or by a zinc finger domain mutant IE2-86 (IE2 Zn mut) **(C),** as described
911 in figure 7. **D)** HFFs were transiently transfected with wild-type pGL2-*PVR* (-571 bp fragment)

promoter luciferase reporter vector, or with 5'-deletions constructs (-470, -343, -281, and -213), together with plasmid vectors containing IE1 and IE2 cDNA, or with pSG5. After 48 h, cells were harvested and luciferase activity was calculated as reported in figure 7. Data represent the mean value from at least four independent experiments ± SE. ns: not significant; * $p<0.05$; ** $p<0.01$; *** $p<0.001$ with Student's t-test.

Supporting Information

Supplementary Figure 1. HCMV AD169 and TR strains induce expression of cell surface MICA. HFFs were grown to subconfluence and then mock-infected or infected with HCMV AD169 and TR at an MOI of 1 PFU/cell, or mock infected. At 4 dpi, cells were fixed and immunostained for MICA ligand, without permeabilization. Immunofluorescence experiments were repeated three times, and representative results are presented. Magnification: 60X.

Supplementary Figure 2. Activation of DDR pathway after HCMV infection. HFFs were infected with the HCMV (AD169) at a MOI of 1 PFU/cell or mock-infected (n.i.) and harvested at 3 dpi. Phospho-histone H2AX (γH2AX) (Ser139) expression levels were evaluated by FACS analysis on cells stained with a specific FITC-conjugated mAb. **A)** A representative experiment of four performed at 3 dpi is shown. **B)** Data are presented as fold induction of γH2AX MFI values in HCMV-infected versus not infected (n.i.) cells, set at 1. Values represent the mean of four independent experiments ± SE. * $p<0.05$ with Student's *t*-test of n.i. versus HCMV-infected cells.

Supplementary Figure 3. Absence of functional ATM does not prevent cell surface expression of MICA, ULBP3 and PVR. AT-/- fibroblasts were mock-infected (n.i.) or infected with HCMV AD169 at an MOI of 1 PFU/cell. At different dpi, cells were harvested and ligand expression was analyzed as in figure 1. A representative experiment out of three is shown.

Supplementary Figure 4. ATM silencing does not affect MICA, ULBP3 and PVR expression. HFFs were transiently transfected with siRNA specific for ATM (siATM) or with a non-targeting siRNA (siCtrl). 24 h later, cells were either uninfected or infected with HCMV AD169 at an MOI of 1 PFU/cell. At 2 dpi, cells and supernatants were harvested and assayed for ligand expression, immunoblot analysis, percentage of IE+ cells, and infectious virus production. **A)** Flow cytometry analysis of MICA, ULBP3 and PVR expression was performed as described in figure 1. Vertical dotted lines indicate the center of the peak for each ligand in not infected-siCtrl transfected cells (thin grey histograms). All panels derive from the same experiment, representative of three. **B)** The levels of ATM protein expression were assayed by immunoblot analysis with a specific antibody. Immunodetection of the p85 subunit of PI-3K was used as a control of protein loading. **C)** The % of IE+ cells was analyzed by flow cytometry on HCMV-infected cells by intracellular staining with a specific anti-IE mAb. **D)** Cell culture supernatants were assayed for infectious virus production by plaque assay. ns: not statistically significant difference with Student's t-test.

Supplementary Figure 5. ATR silencing does not affect MICA, ULBP3 and PVR expression. HFFs were transfected with siRNA specific for ATR (siATR) or with a non-targeting siRNA (siCtrl), infected and harvested as described in Fig. S4. **A)** Flow cytometry analysis of

MICA, ULBP3 and PVR expression was performed as described in figure 1. Vertical dotted lines indicate the center of the peak for each ligand in not infected-siCtrl transfected cells (thin grey histograms). All panels derive from the same experiment, representative of three. **B**) The levels of ATR protein expression were assayed by immunoblot analysis with a specific antibody. Immunodetection of the p85 subunit of PI-3K was used as a control of protein loading. **C)** The % of IE+ cells was analyzed by flow cytometry on HCMV-infected cells by intracellular staining with a specific anti-IE mAb. **D)** Cell culture supernatants were assayed for infectious virus production by plaque assay. ns: not statistically significant difference with Student's t-test.

Supplementary Figure 6. DNA-PK silencing does not affect MICA, ULBP3 and PVR expression. HFFs were transfected with siRNA specific for DNA-PK (siDNA-PK) or with a non-targeting siRNA (siCtrl), infected and harvested as described in Fig. S4. **A)** Flow cytometry analysis of MICA, ULBP3 and PVR expression as described in figure 1. Vertical dotted lines indicate the center of the peak for each ligand in not infected-siCtrl transfected cells (thin grey histograms). All panels derive from the same experiment, representative of three. **B**) The levels of DNA-PK protein expression were assayed by immunoblot analysis with a specific antibody. Immunodetection of the p85 subunit of PI-3K was used as a control of protein loading. **C)** The % of IE+ cells was analyzed by flow cytometry on HCMV-infected cells by intracellular staining with a specific anti-IE mAb. **D)** Cell culture supernatants were assayed for infectious virus production by plaque assay. ns: not statistically significant difference with Student's t-test.

Acknowledgements

We wish to thank Jay A. Nelson and Michael A. Jarvis M for the TR BAC and the IE2-86 zinc finger mutant; Giuseppe Gerna for VR-1814 strain; Andrea Gallina for ARPE-19 cells and Tiziana Bruno and Maurizio Fanciulli for AT-/- fibroblasts; Tim Kowalik for recombinant IE1 adenovirus; Marco Colonna for the anti-PVR mAb SKII.4; Jack D. Bui for pGL-3 MICA promoter vector, and Günter Bernhardt for PVR promoter progressive deletions. We wish to thank members of the Santoni laboratory for discussions.

Author Contributions

Conceived and designed the experiments: BP, CF, VDO, MC, SL, GG, AS, CC. Performed the experiments: BP, CF, AL, CC. Analyzed the data: BP, CF, MC, CC. Contributed reagents/materials/analysis tools: CF, VDO, AL, AZ, MC, SL, GG, AS. Wrote the paper: BP, CF, GG, AS, CC.

Funding

This work was funded by grants from the Pasteur Institute - Cenci-Bolognetti Foundation and the “Sapienza” University of Rome to C.C., the Center of Excellence for Biology and Molecular Medicine (BEMM), the Italian Ministry of University and Research (MIUR) (PRIN 2010-11, grant no. 2010PHT9NF to G.G. and Ex-60% to A.L. and G.G.; PRIN 2012 grant no. 2012SNMJRL to SL; PRIN 2012 grant no. 20127MFYBR to VDO). The funders had no role in study design, data collection and analysis, decision to publish, or preparation of the manuscript. Nostro PRIN?

Table S1. Statistical analysis of the results obtained for MICA mRNA and cell surface expression on HFF cells transduced with the indicated recombinant AdV.

MICA (mRNA)	**-**	*LacZ*	*IE72*	*IE86*	*IE72+IE86*
-	/	ns	ns	0.026	0.004
LacZ		/	ns	0.022	0.003
IE72			/	0.025	0.003
IE86				/	ns
IE72+IE86					/
MICA (cell surface)					
-	/	ns	ns	0.031	0.044
LacZ		/	ns	0.023	0.035
IE72			/	0.025	ns
IE86				/	ns
IE72+IE86					/

Table S2. Statistical analysis of the results obtained for PVR mRNA and cell surface expression on HFF cells transduced with the indicated recombinant AdV.

VR (mRNA)	**-**	*LacZ*	*IE72*	*IE86*	*IE72+IE86*
-	/	ns	ns	ns	0.038
LacZ		/	ns	0.021	0.022
IE72			/	ns	0.025
IE86				/	0.019
IE72+IE86					/
PVR (cell surface)					
-	/	ns	0.0006	0.030	0.0008
LacZ		/	0.005	0.009	0.003
IE72			/	ns	0.003
IE86				/	0.024
IE72+IE86					/

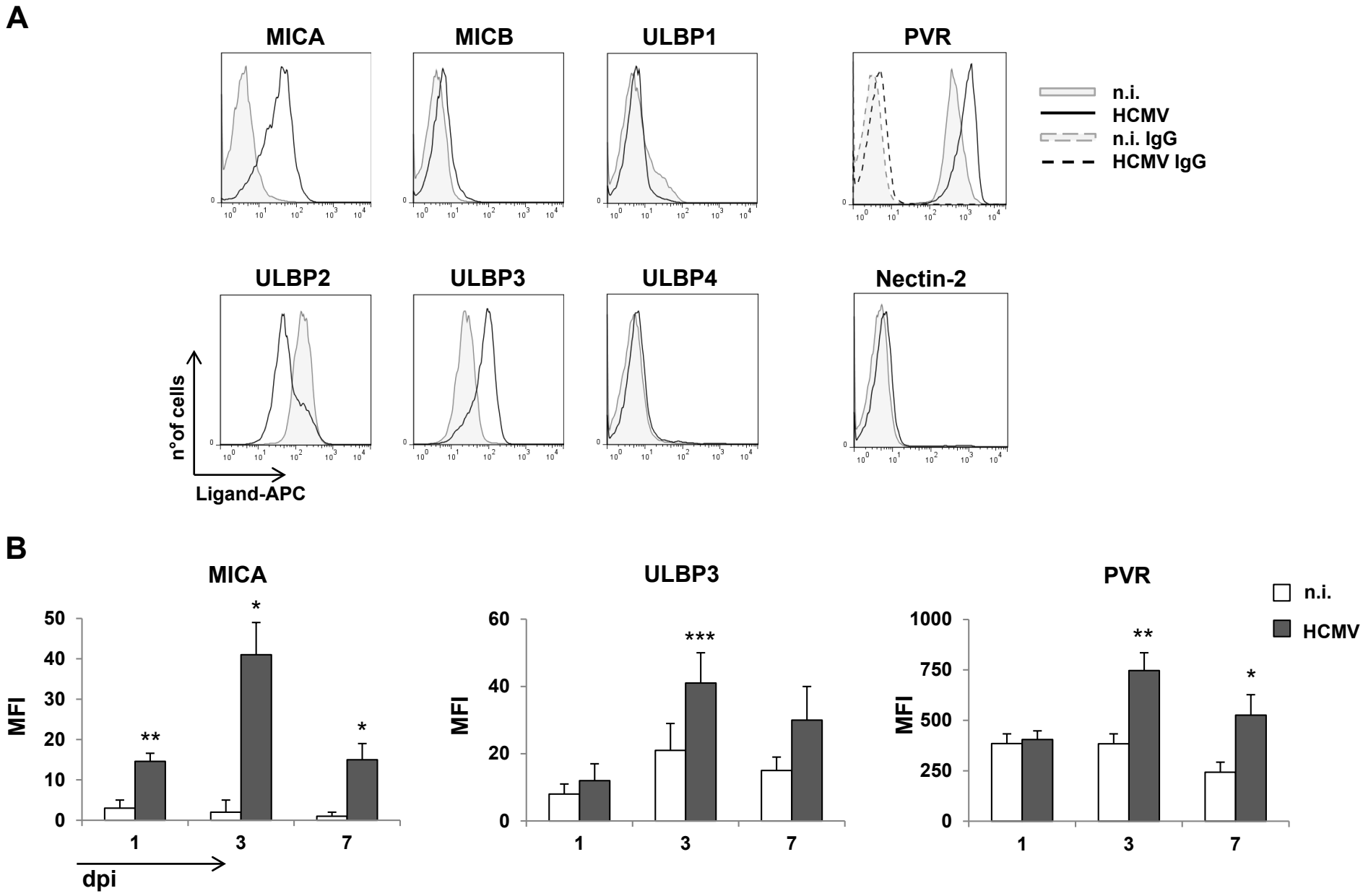
A
MICA
MICB
ULBP1
PVR
ULBP2
ULBP3
ULBP4
Nectin-2
n°of cells
Ligand-APC
n.i.
HCMV
n.i. IgG
HCMV IgG
B
MICA
ULBP3
PVR
MFI
dpi
1
3
7
n.i.
HCMV

Fig. 1

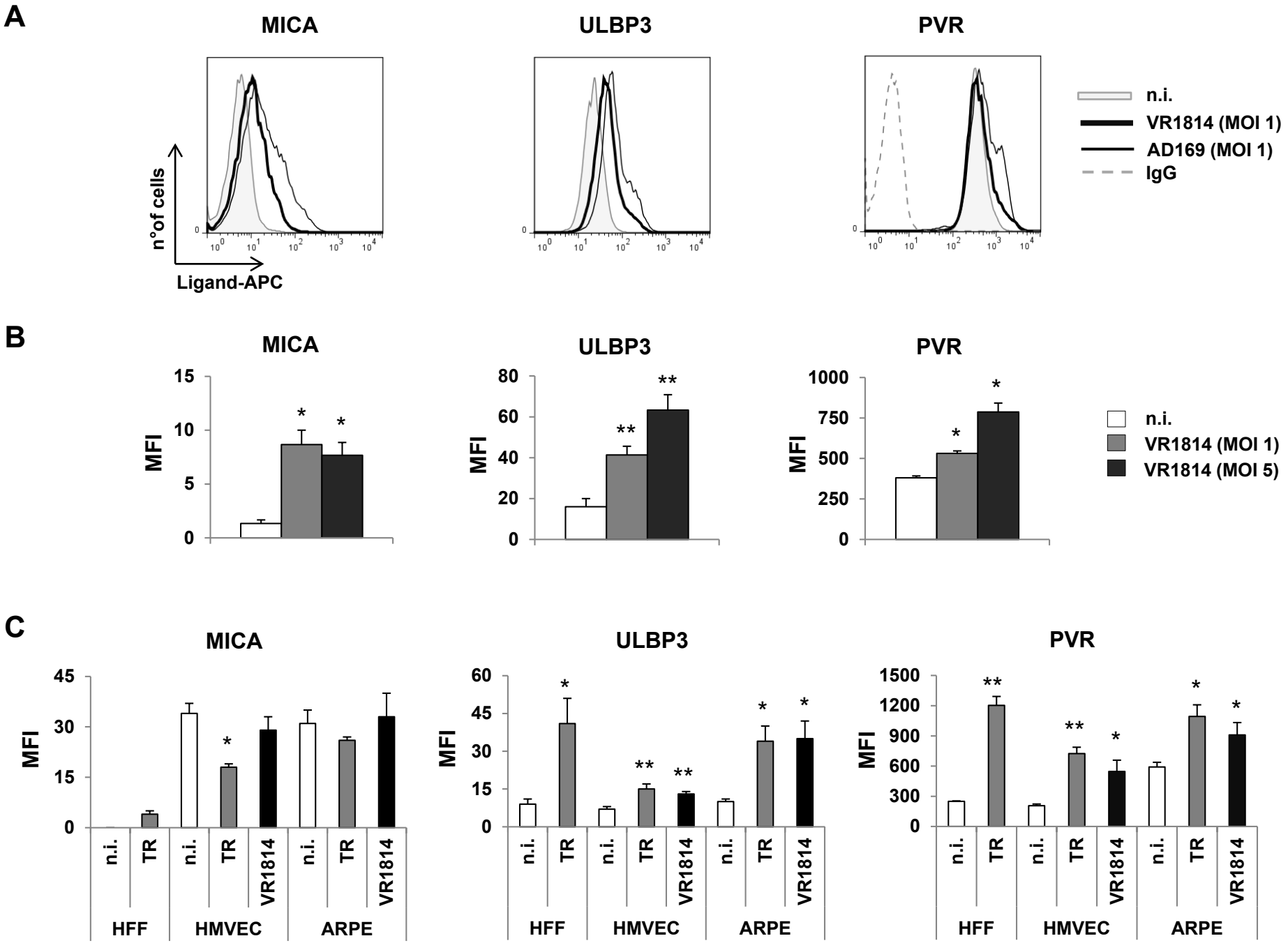
A
MICA
ULBP3
PVR
n°of cells
Ligand-APC
n.i.
VR1814 (MOI 1)
AD169 (MOI 1)
IgG
B
MICA
ULBP3
PVR
MFI
n.i.
VR1814 (MOI 1)
VR1814 (MOI 5)
C
MICA
ULBP3
PVR
MFI
n.i.
TR
VR1814
HFF
HMVEC
ARPE

Fig. 2

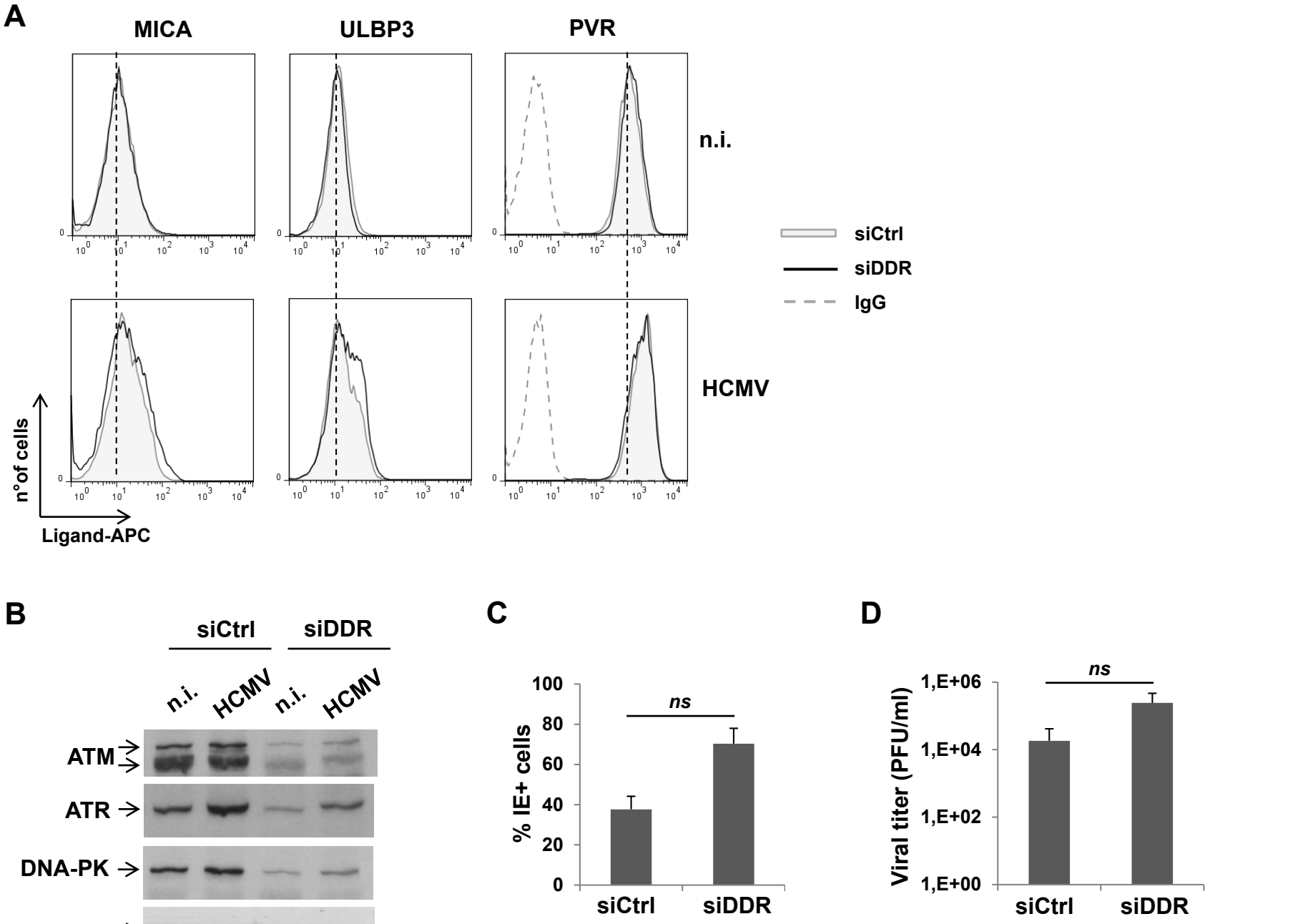
A
MICA
ULBP3
PVR
n.i.
HCMV
siCtrl
siDDR
IgG
n°of cells
Ligand-APC
B
siCtrl
siDDR
n.i.
HCMV
n.i.
HCMV
ATM
ATR
DNA-PK
p85
C
% IE+ cells
100
80
60
40
20
0
ns
siCtrl
siDDR
D
Viral titer (PFU/ml)
1,E+06
1,E+04
1,E+02
1,E+00
ns
siCtrl
siDDR

Fig. 3

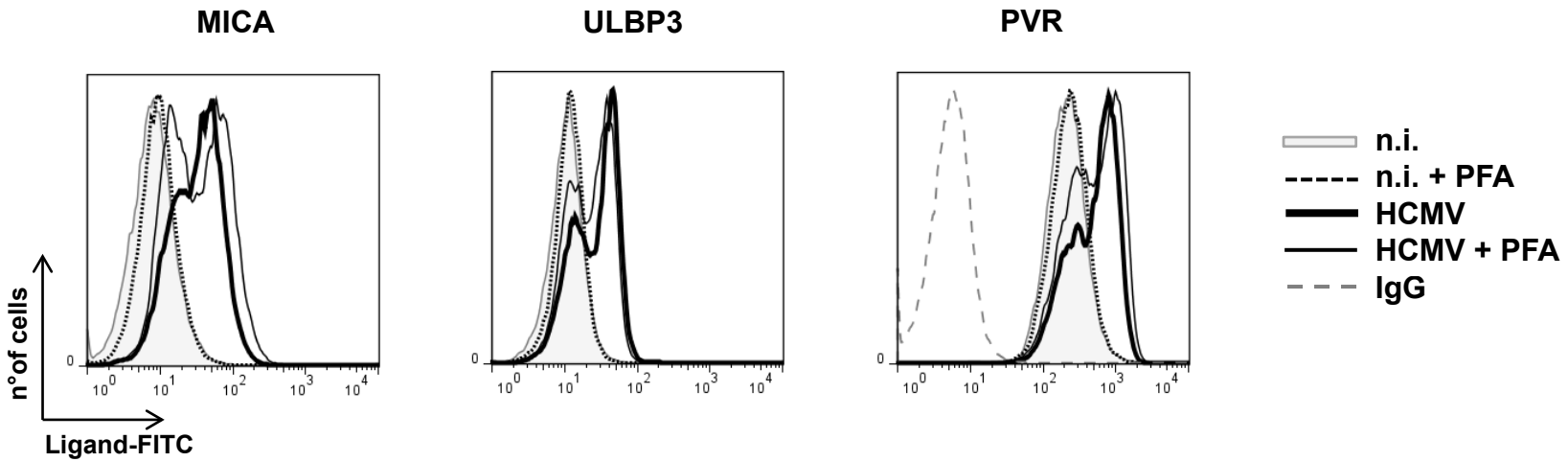
MICA
ULBP3
PVR
n°of cells
Ligand-FITC
n.i.
n.i. + PFA
HCMV
HCMV + PFA
IgG

Fig. 4

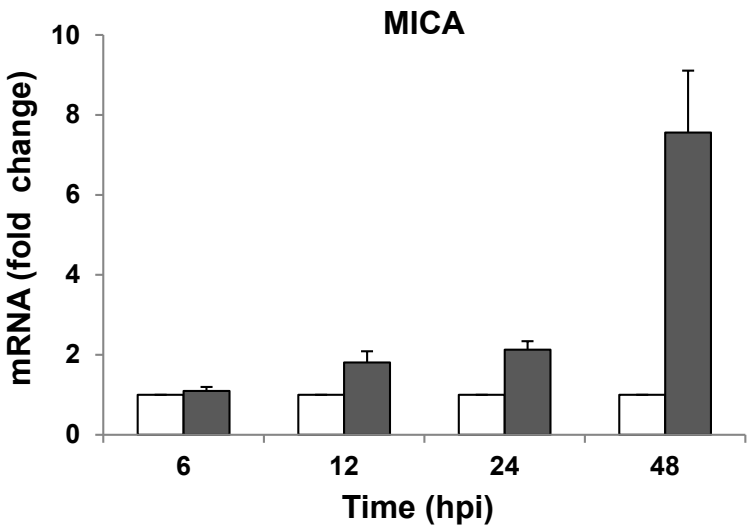
MICA
mRNA (fold change)
10
8
6
4
2
0
6
12
24
48
Time (hpi)

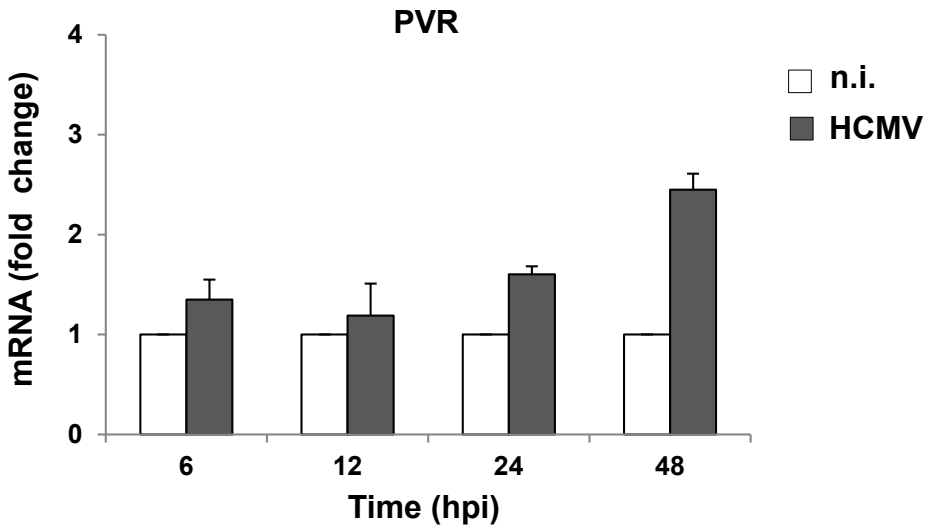
PVR
mRNA (fold change)
4
3
2
1
0
6
12
24
48
Time (hpi)
n.i.
HCMV

Fig. 5

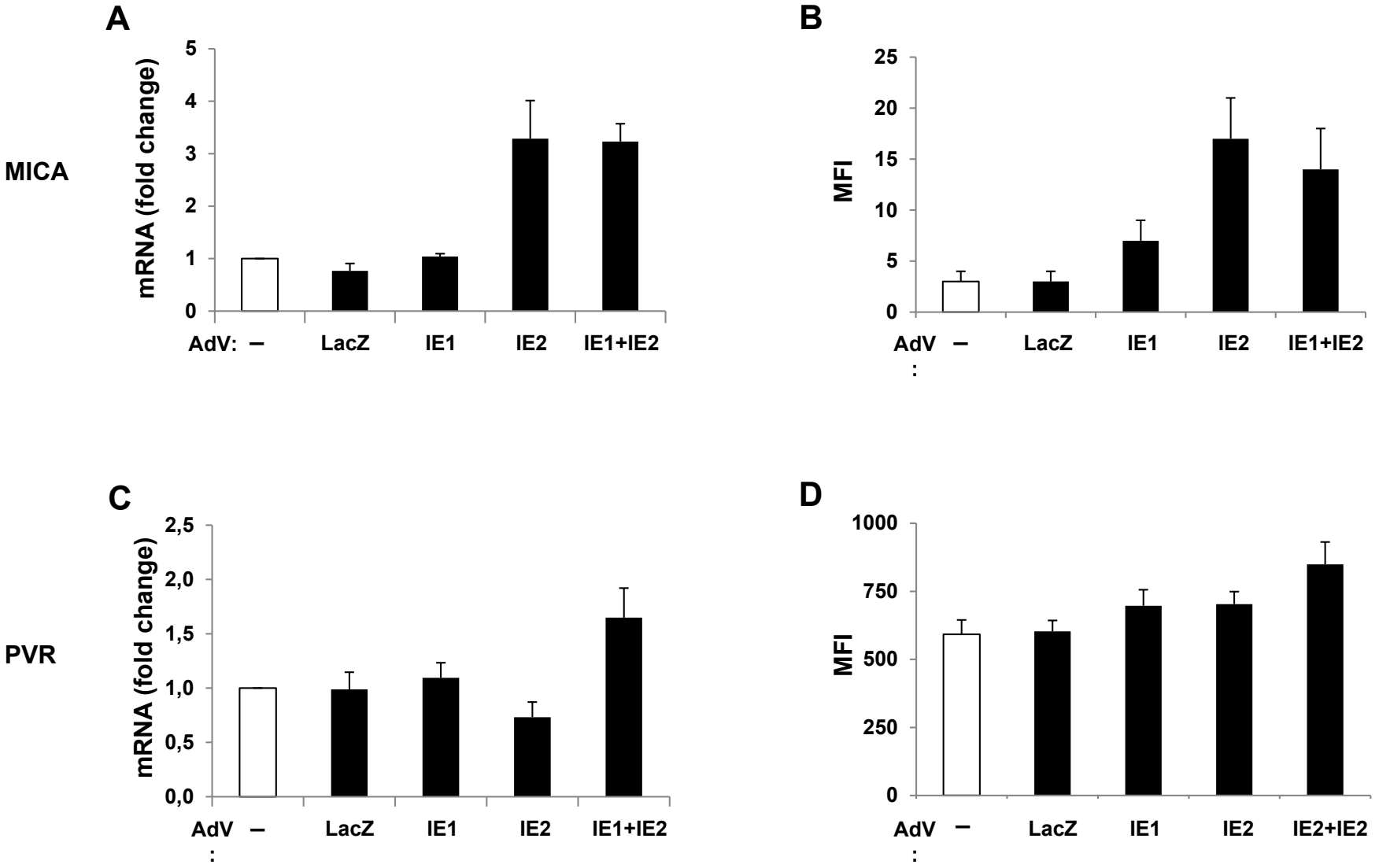
A
B
MICA
mRNA (fold change)
MFI
AdV: –
LacZ
IE1
IE2
IE1+IE2
C
D
PVR
mRNA (fold change)
MFI
AdV: –
LacZ
IE1
IE2
IE2+IE2

Fig. 6

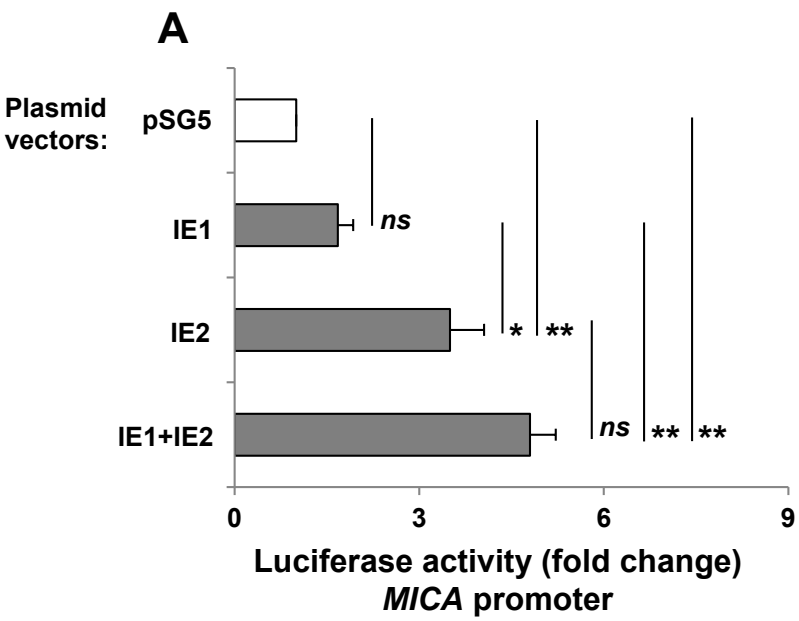
A
Plasmid vectors:
pSG5
IE1
IE2
IE1+IE2
ns
*
**
ns
**
**
0
3
6
9
Luciferase activity (fold change)
MICA promoter

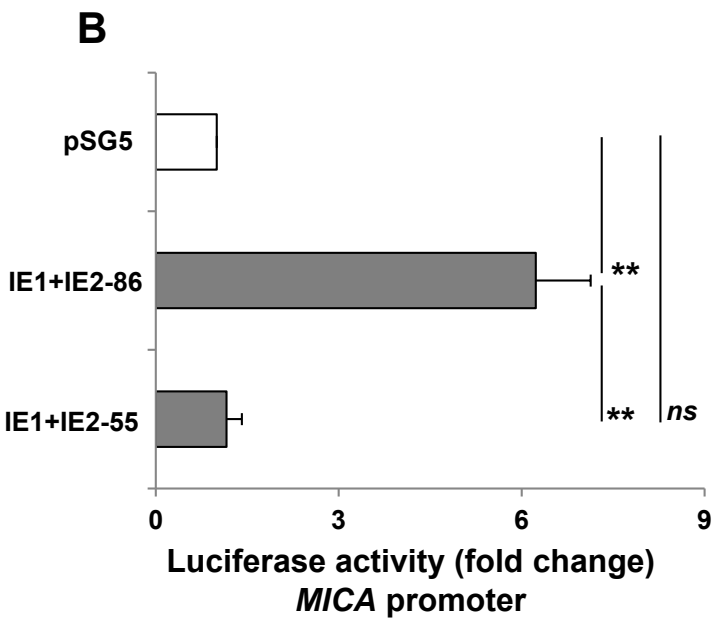
B
pSG5
IE1+IE2-86
IE1+IE2-55
**
**
ns
0
3
6
9
Luciferase activity (fold change)
MICA promoter

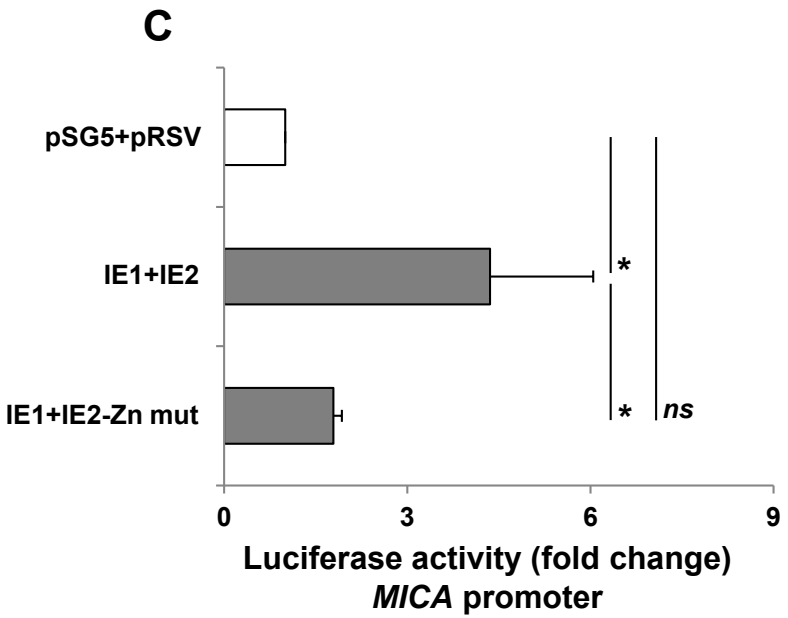
C
pSG5+pRSV
IE1+IE2
IE1+IE2-Zn mut
*
*
ns
0
3
6
9
Luciferase activity (fold change)
MICA promoter

Fig. 7

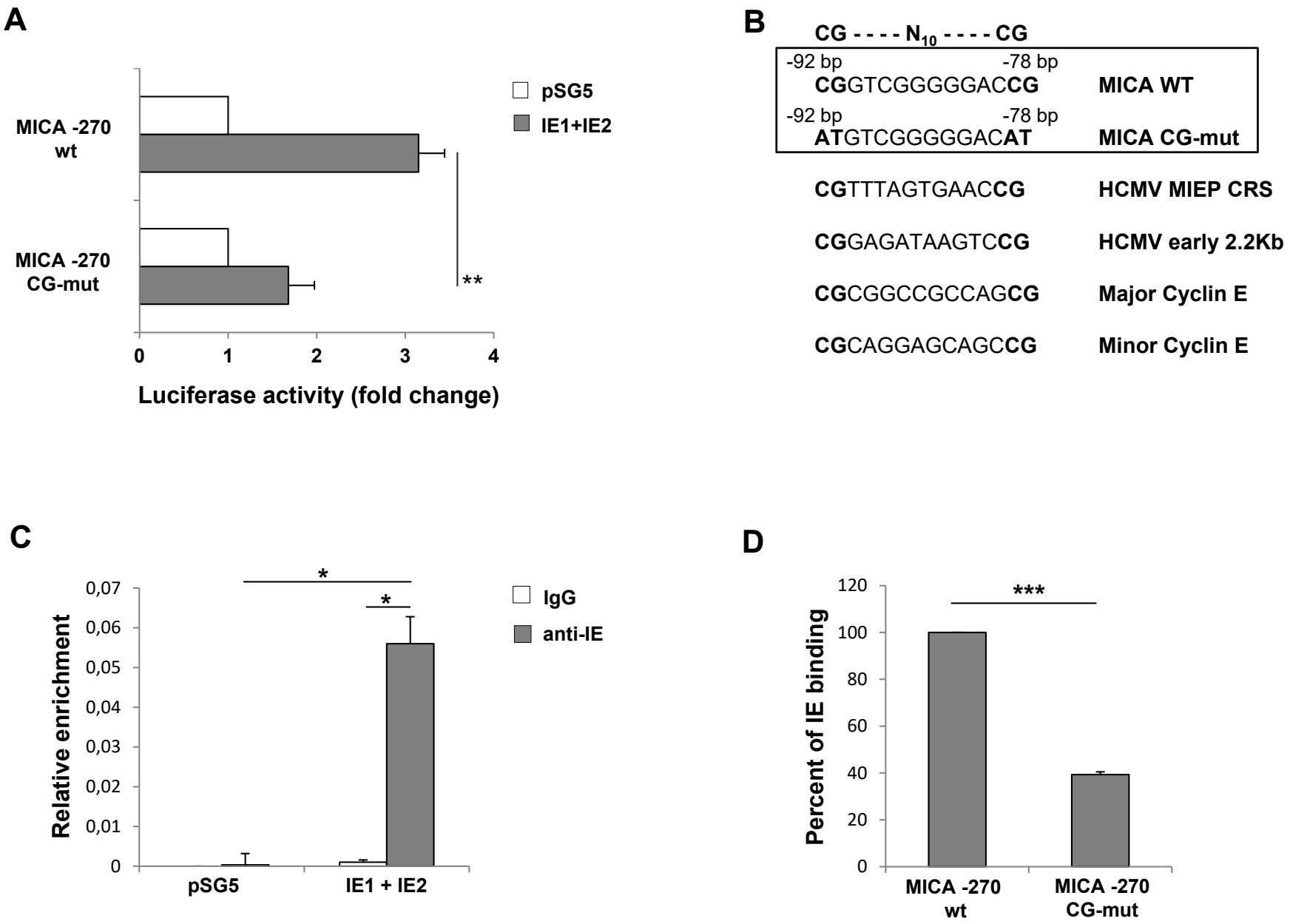
A
MICA -270 wt
MICA -270 CG-mut
pSG5
IE1+IE2
**
0
1
2
3
4
Luciferase activity (fold change)
B
CG - - - - N10 - - - - CG
-92 bp
-78 bp
CGGTCGGGGGACCG
MICA WT
-92 bp
-78 bp
ATGTCGGGGGACAT
MICA CG-mut
CGTTTAGTGAACCG
HCMV MIEP CRS
CGGAGATAAGTCCG
HCMV early 2.2Kb
CGCGGCCGCCAGCG
Major Cyclin E
CGCAGGAGCAGCCG
Minor Cyclin E
C
Relative enrichment
0,07
0,06
0,05
0,04
0,03
0,02
0,01
0
*
*
IgG
anti-IE
pSG5
IE1 + IE2
D
Percent of IE binding
120
100
80
60
40
20
0
***
MICA -270 wt
MICA -270 CG-mut

Fig. 8

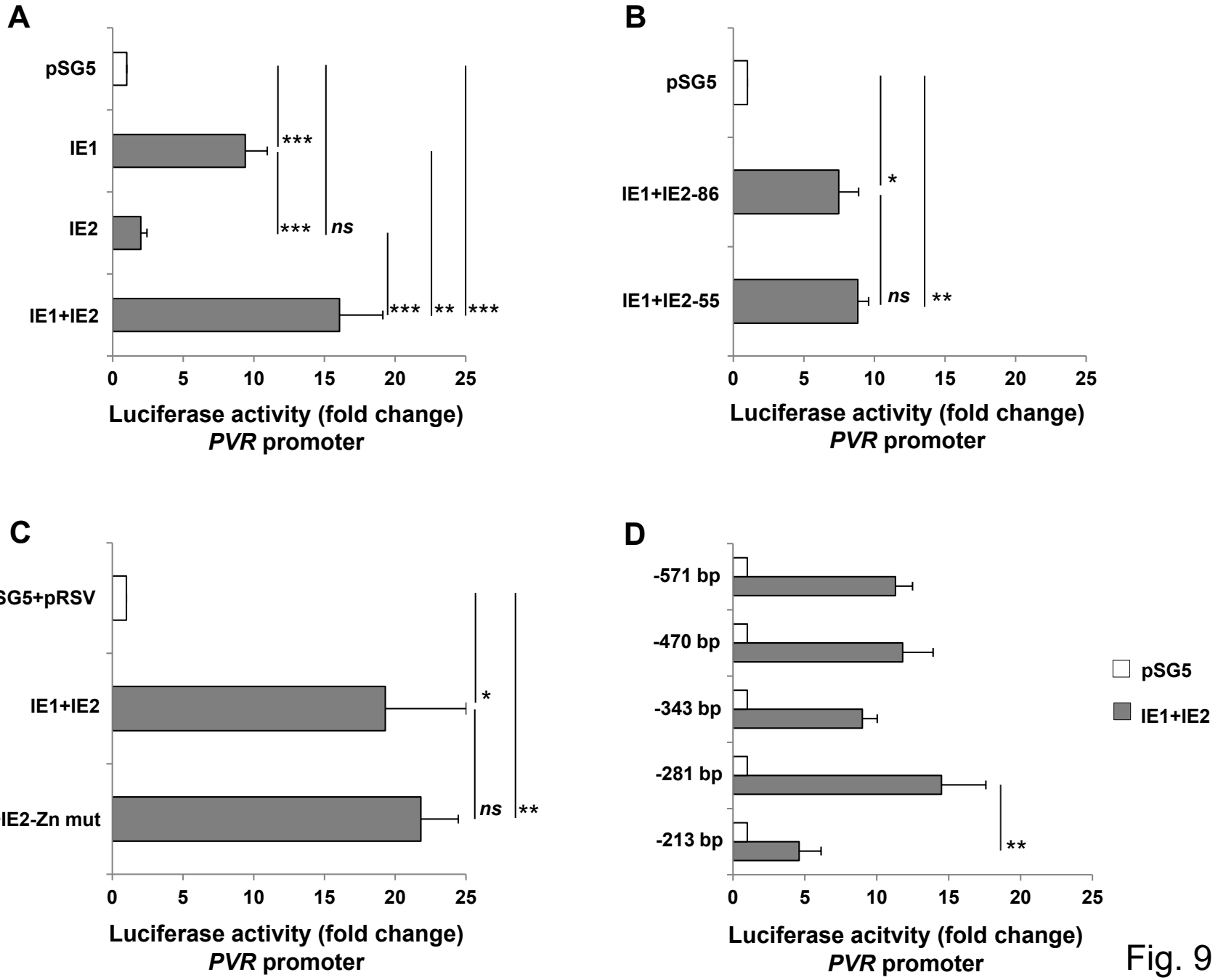
A
pSG5
IE1
IE2
IE1+IE2
***
***
ns
***
**
***
0
5
10
15
20
25
Luciferase activity (fold change)
PVR promoter
B
pSG5
IE1+IE2-86
IE1+IE2-55
*
ns
**
0
5
10
15
20
25
Luciferase activity (fold change)
PVR promoter
C
pSG5+pRSV
IE1+IE2
IE1+IE2-Zn mut
*
ns
**
0
5
10
15
20
25
Luciferase activity (fold change)
PVR promoter
D
-571 bp
-470 bp
-343 bp
-281 bp
-213 bp
**
pSG5
IE1+IE2
0
5
10
15
20
25
Luciferase acitvity (fold change)
PVR promoter

Fig. 9

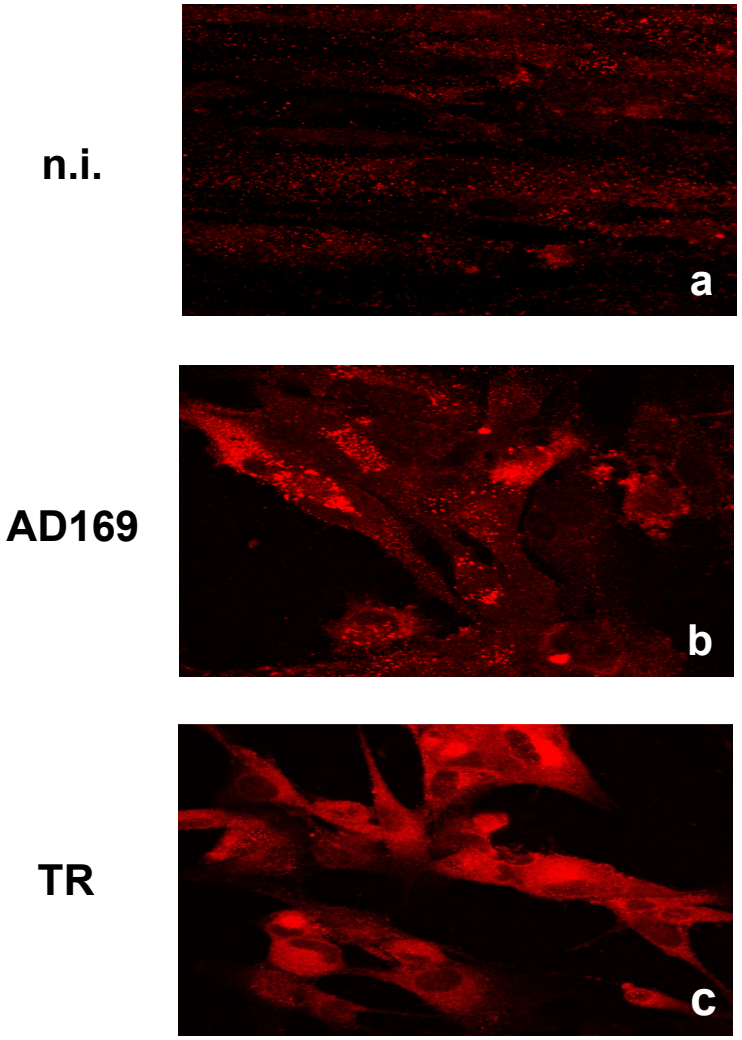

Fig. S1

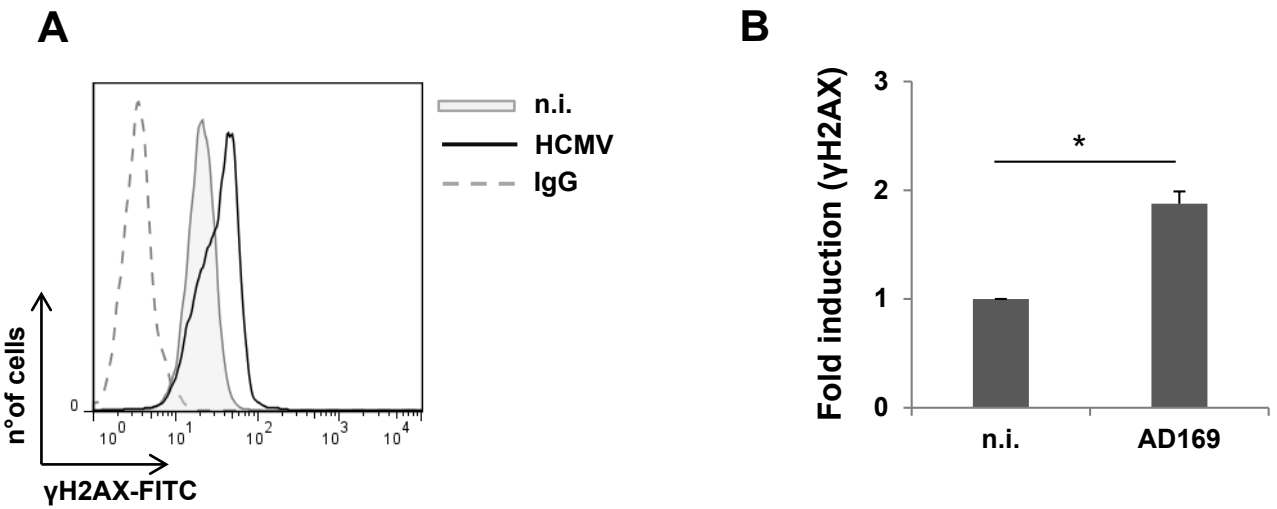
A
n.i.
HCMV
IgG
n°of cells
0
10^0
10^1
10^2
10^3
10^4
γH2AX-FITC
B
Fold induction (γH2AX)
3
2
1
0
*
n.i.
AD169

Fig. S2

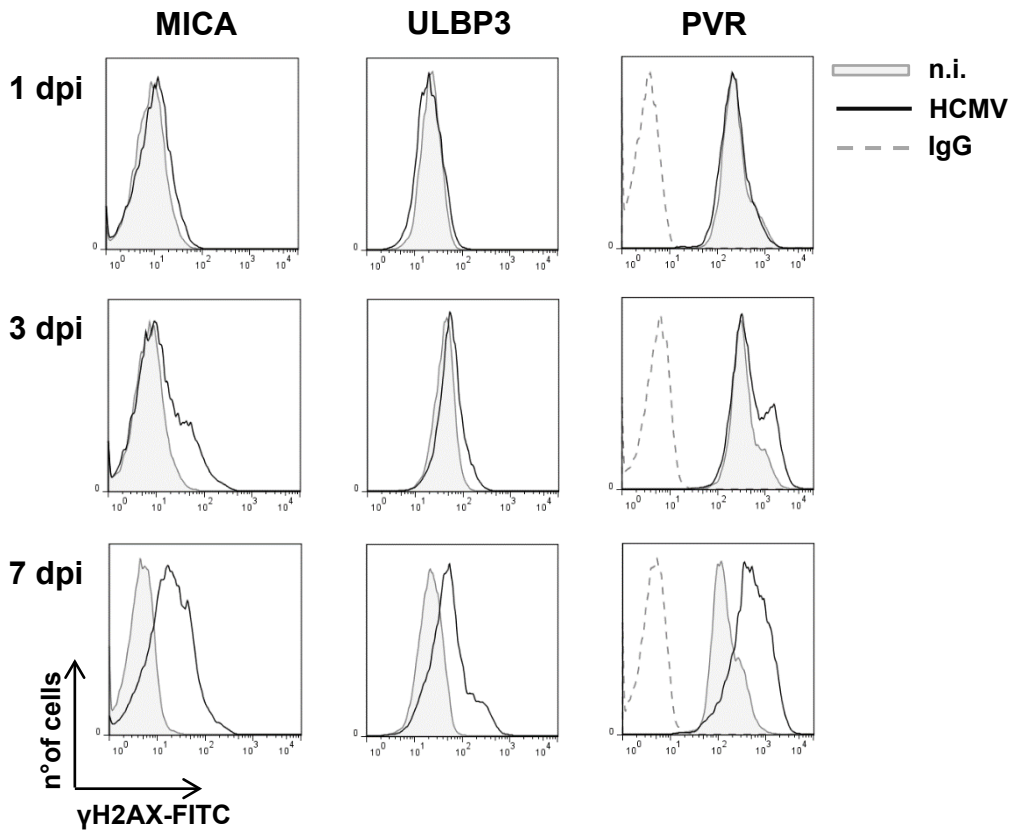
MICA
ULBP3
PVR
1 dpi
3 dpi
7 dpi
n.i.
HCMV
IgG
n°of cells
γH2AX-FITC

Fig. S3

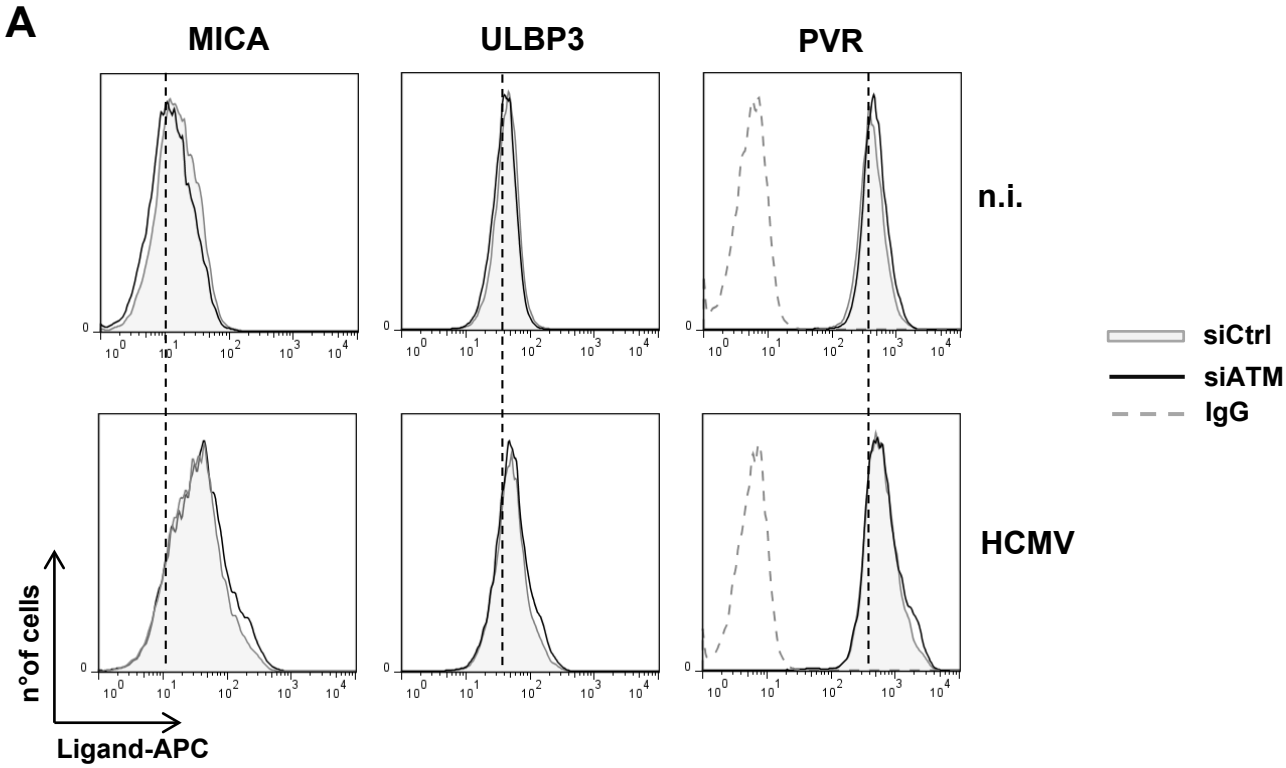
A
MICA
ULBP3
PVR
n.i.
HCMV
siCtrl
siATM
IgG
n°of cells
Ligand-APC

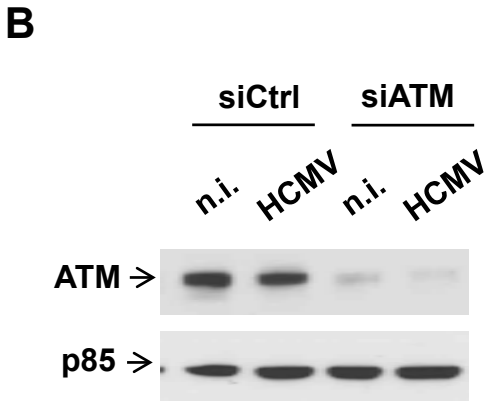
B
siCtrl
siATM
n.i.
HCMV
n.i.
HCMV
ATM
p85

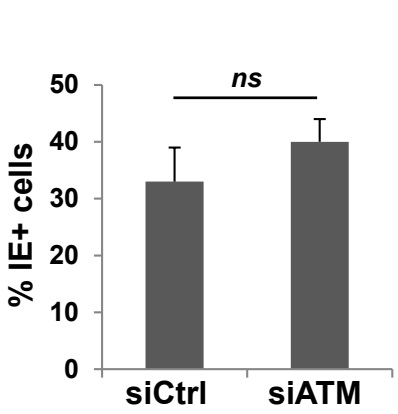
C
ns
% IE+ cells
50
40
30
20
10
0
siCtrl
siATM

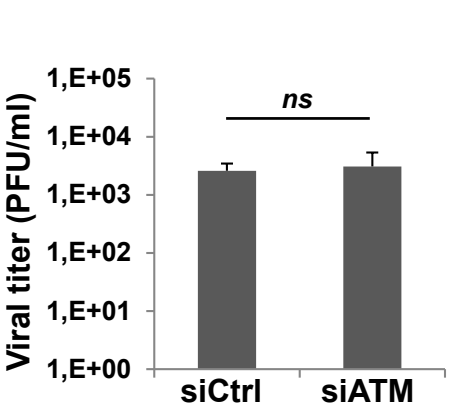
D
ns
Viral titer (PFU/ml)
1,E+05
1,E+04
1,E+03
1,E+02
1,E+01
1,E+00
siCtrl
siATM

Fig. S4

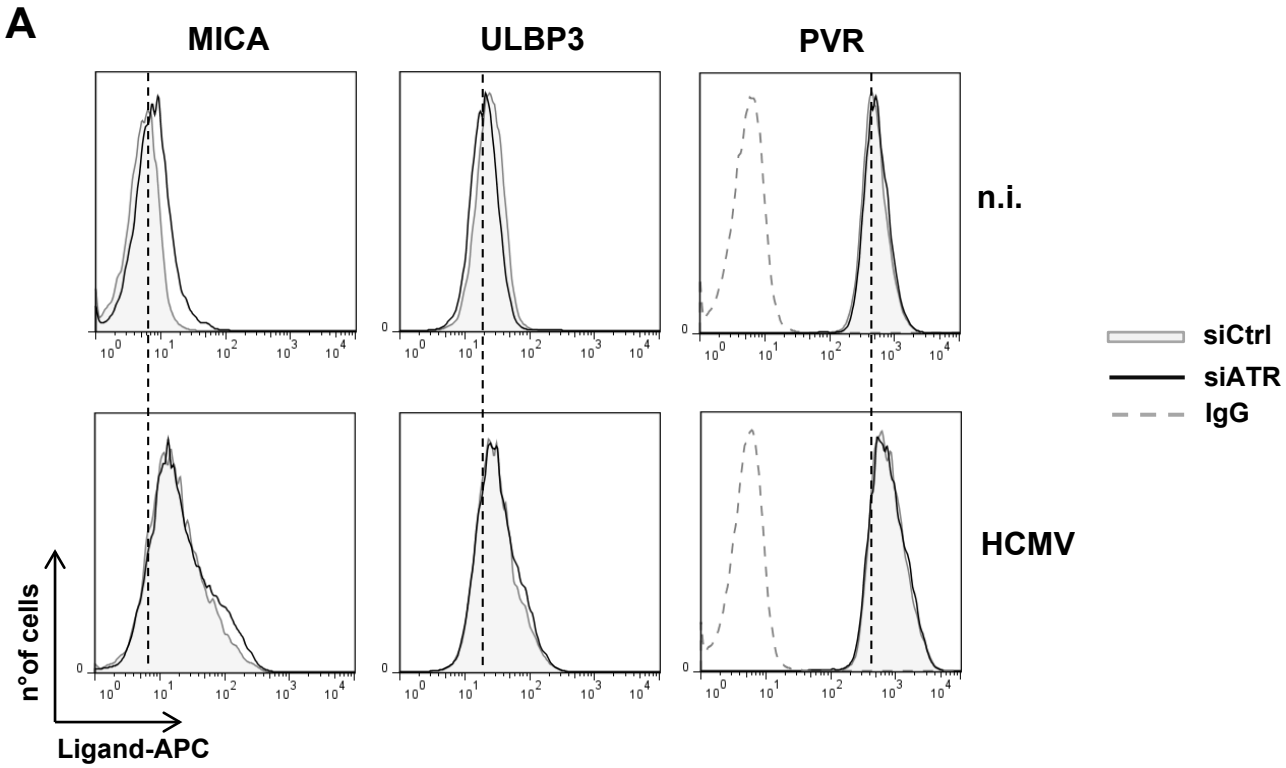
A
MICA
ULBP3
PVR
n.i.
HCMV
siCtrl
siATR
IgG
n°of cells
Ligand-APC

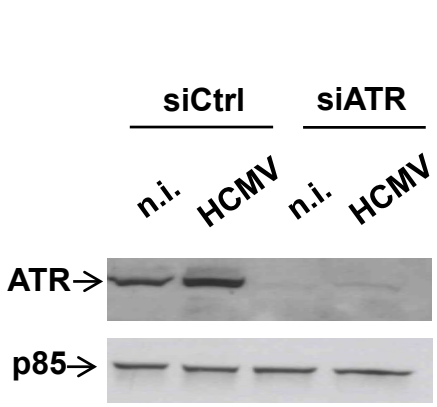
B
siCtrl
siATR
n.i.
HCMV
n.i.
HCMV
ATR
p85

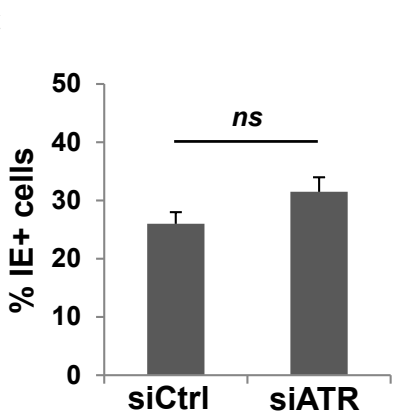
C
% IE+ cells
50
40
30
20
10
0
ns
siCtrl
siATR

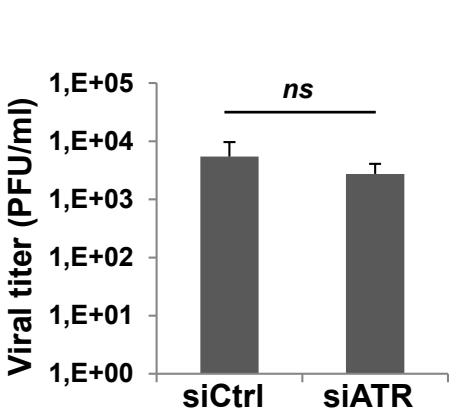
D
Viral titer (PFU/ml)
1,E+05
1,E+04
1,E+03
1,E+02
1,E+01
1,E+00
ns
siCtrl
siATR

Fig. S5

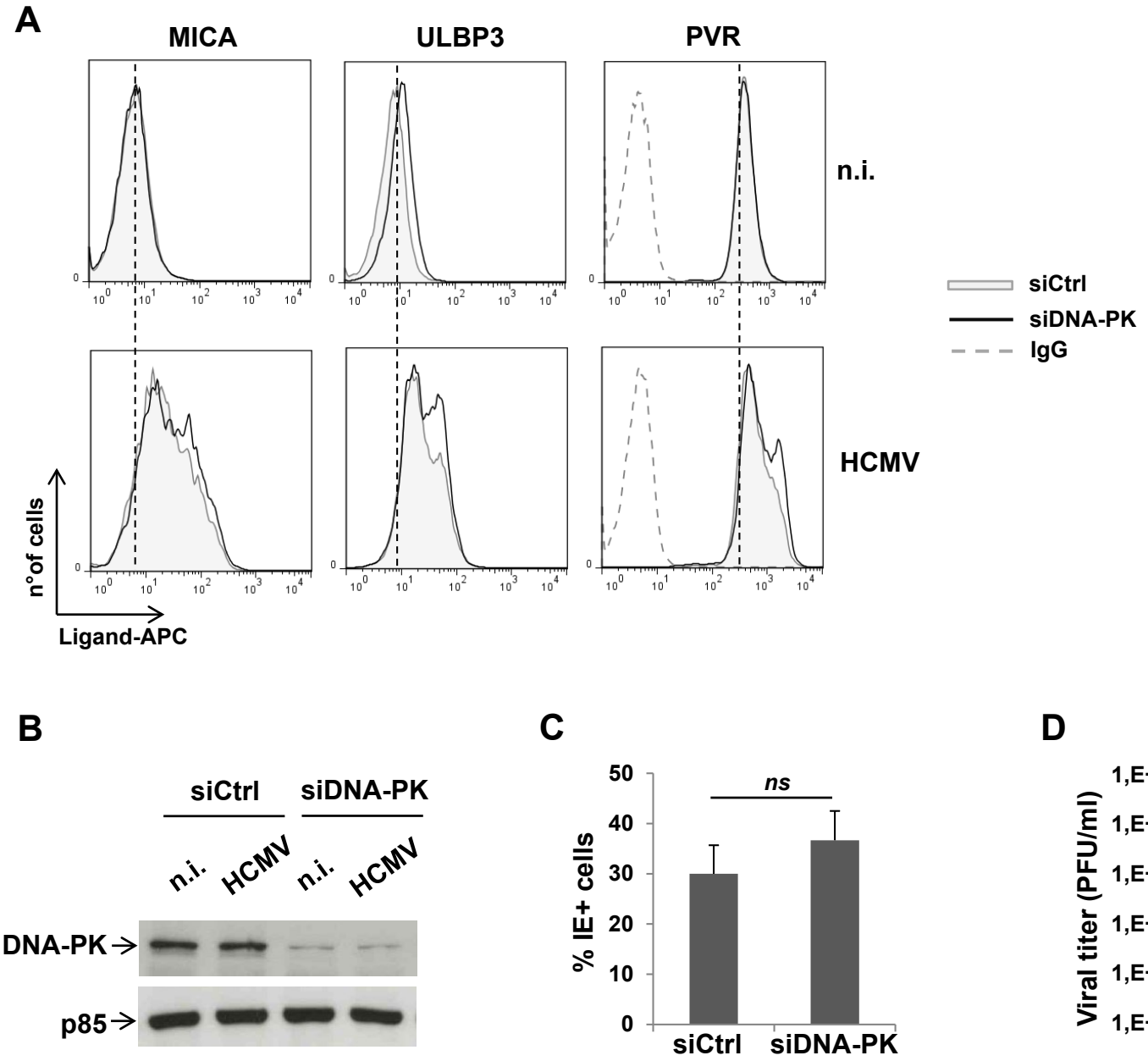
A
MICA
ULBP3
PVR
n.i.
HCMV
siCtrl
siDNA-PK
IgG
n°of cells
Ligand-APC
B
siCtrl
siDNA-PK
n.i.
HCMV
n.i.
HCMV
DNA-PK
p85
C
% IE+ cells
50
40
30
20
10
0
ns
siCtrl
siDNA-PK
D
Viral titer (PFU/ml)
1,E+05
1,E+04
1,E+03
1,E+02
1,E+01
1,E+00
ns
siCtrl
siDNA-PK

Fig. S6